Active Noise Control: A Tutorial Review

SEN M. KUO AND DENNIS R. MORGAN, SENIOR MEMBER, IEEE

Active noise control (ANC) is achieved by introducing a canceling "antinoise" wave through an appropriate array of secondary sources. These secondary sources are interconnected through an electronic system using a specific signal processing algorithm for the particular cancellation scheme. ANC has application to a wide variety of problems in manufacturing, industrial operations, and consumer products. The emphasis of this paper is on the practical aspects of ANC systems in terms of adaptive signal processing and digital signal processing (DSP) implementation for real-world applications.

In this paper, the basic adaptive algorithm for ANC is developed and analyzed based on single-channel broad-band feedforward control. This algorithm is then modified for narrow-band feedforward and adaptive feedback control. In turn, these single-channel ANC algorithms are expanded to multiple-channel cases. Various online secondary-path modeling techniques and special adaptive algorithms, such as lattice, frequency-domain, subband, and recursive-least-squares, are also introduced. Applications of these techniques to actual problems are highlighted by several examples.

Keywords*—*Active noise control, active vibration control, adaptive noise cancellation, adaptive systems, digital signal processing (DSP) applications.

I. INTRODUCTION

A. Overview

Acoustic noise problems become more and more evident as increased numbers of industrial equipment such as engines, blowers, fans, transformers, and compressors are in use. The traditional approach to acoustic noise control uses passive techniques such as enclosures, barriers, and silencers to attenuate the undesired noise [1], [2]. These passive silencers are valued for their high attenuation over a broad frequency range; however, they are relatively large, costly, and ineffective at low frequencies. Mechanical vibration is another related type of noise that commonly creates problems in all areas of transportation and manufacturing, as well as with many household appliances.

Active noise control (ANC) [3]–[6] involves an electroacoustic or electromechanical system that cancels the primary (unwanted) noise based on the principle of superposition; specifically, an antinoise of equal amplitude and opposite phase is generated and combined with the primary noise, thus resulting in the cancellation of both noises. The ANC system efficiently attenuates low-frequency noise where passive methods are either ineffective or tend to be very expensive or bulky. ANC is developing rapidly because it permits improvements in noise control, often with potential benefits in size, weight, volume, and cost.

The design of acoustic ANC utilizing a microphone and an electronically driven loudspeaker to generate a canceling sound was first proposed in a 1936 patent by Lueg [7]. Since the characteristics of the acoustic noise source and the environment are time varying, the frequency content, amplitude, phase, and sound velocity of the undesired noise are nonstationary. An ANC system must therefore be adaptive in order to cope with these variations. Adaptive filters [8]–[16] adjust their coefficients to minimize an error signal and can be realized as (transversal) finite impulse response (FIR), (recursive) infinite impulse response (IIR), lattice, and transform-domain filters. The most common form of adaptive filter is the transversal filter using the least-mean-square (LMS) algorithm. An early duct cancellation system based on adaptive filter theory was developed in [17] and [18].

It is desirable for the noise canceler to be digital [19], [20], where signals from electroacoustic or electromechanical transducers are sampled and processed in real time using digital signal processing (DSP) systems. In the 1980's, development of DSP chips enabled low-cost implementation of powerful adaptive algorithms [21] and encouraged widespread development and application of ANC systems [22]. The continuous progress of ANC involves the development of improved adaptive signal processing algorithms, transducers, and DSP hardware. More sophisticated algorithms allow faster convergence and greater noise attenuation and are more robust to interference. The development of improved DSP hardware allows these more sophisticated algorithms to be implemented in real time to improve system performance.

In this paper, noise is defined as any kind of undesirable disturbance, whether it is borne by electrical, acoustic, vibration, or any other kind of media. Therefore, ANC algorithms introduced in this paper can be applied to different types of noise using appropriate sensors and secondary sources. For electrical engineers involved in the

Manuscript received June 1, 1997; revised December 18, 1998.

S. M. Kuo is with the Department of Electrical Engineering, Northern Illinois University, DeKalb, IL 60115 USA.

D. R. Morgan is with Bell Laboratories, Lucent Technologies, Murray Hill, NJ 07974-0636 USA.

Publisher Item Identifier S 0018-9219(99)04043-8.

development of ANC systems, [3], [5], and [6] provide excellent introduction to acoustics and vibration.

B. Current Applications

ANC is an attractive means to achieve large amounts of noise reduction in a small package, particularly at low frequencies. Many applications of ANC involving real and simulated experiments are introduced in [4]. Current applications for ANC include attenuation of unavoidable noise in the following end equipment.

1) Automotive: Including electronic mufflers for exhaust and induction systems, noise attenuation inside vehicle passenger compartments, active engine mounts, and so on.

2) Appliances: Including air-conditioning ducts, air conditioners, refrigerators, kitchen exhaust fans, washing machines, furnaces, dehumidifiers, lawn mowers, vacuum cleaners, headboards, room isolation, and so on.

3) Industrial: Fans, air ducts, chimneys, transformers, power generators, blowers, compressors, pumps, chain saws, wind tunnels, noisy plants (at noise sources or many local quiet zones), public phone booths, office cubicle partitions, ear protectors, headphones, and so on.

4) Transportation: Airplanes, ships, boats, pleasure motorboats, helicopters, snowmobiles, motorcycles, diesel locomotives, and so on.

C. Performance Evaluation and Practical Considerations

When ANC is deployed in real applications, many practical problems arise and need to be addressed [23]. An approach to adaptive ANC performance analysis that involves a hierarchy of techniques, starting with an ideal simplified problem and progressively adding practical constraints and other complexities, is essential [24]. Performance analysis resolves the following issues: 1) the fundamental performance limitations; 2) the practical constraints that limit performance; 3) performance balanced against complexity; and 4) how to determine a practical design architecture. At each step, a degree of confidence is gained and a benchmark is established for comparison and cross checking with the next level of complexity.

In order to be suitable for industrial use, the ANC system must have certain properties [25]: 1) maximum efficiency over the largest frequency band possible to cancel a wide range of noise; 2) autonomy with regard to the installation, so that the system could be built and preset in the manufacturing area and then inserted on site; 3) self adaptability of the system in order to deal with any variations in the physical parameters (temperature, airflow speed, etc.); and 4) robustness and reliability of the different elements of the system and simplification of the control electronics.

D. Paper Outline

ANC is based on either feedforward control, where a coherent reference noise input is sensed before it propagates past the secondary source, or feedback control [26], [27], where the active noise controller attempts to cancel the noise without the benefit of an "upstream" reference input. Structures for feedforward ANC are classified into 1) broad-band adaptive feedforward control with a reference sensor, which will be discussed in Section II, and 2) narrow-band adaptive feedforward control with a reference sensor that is not influenced by the control field (e.g., tachometer), which will be presented in Section III. In Section IV, the concept of adaptive feedback ANC will be developed from the standpoint of reference signal synthesis, thereby providing a link to the feedforward systems in previous sections. In Section V, these single-channel ANC systems will be expanded to multiple-channel cases. Section VI will introduce various online secondary-path modeling techniques. Section VII will introduce various special ANC algorithms such as lattice ANC, frequency-domain ANC, subband ANC, and recursive-least-squares (RLS). Finally, several examples applying ANC to real-world problems will be highlighted in Section VIII.

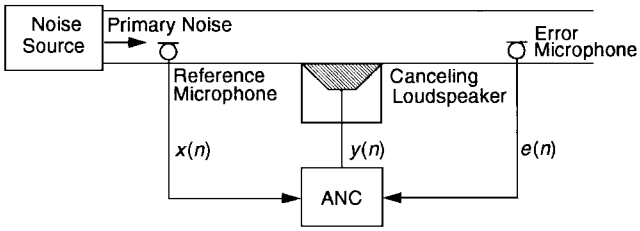

Fig. 1. Single-channel broad-band feedforward ANC system in a duct.

II. Broad-Band Feedforward ANC

This section considers broad-band feedforward ANC systems that have a single reference sensor, single secondary source, and single error sensor. This genre will be exemplified by the single-channel duct-acoustic ANC system shown in Fig. 1, where the reference input is picked up by a microphone. The reference signal is processed by the ANC system to generate the control signal to drive a loudspeaker. The error microphone is used to monitor the performance of the ANC system. The objective of the controller is to minimize the measured acoustic noise. Note that this setup is only used as an example of broad-band ANC; the general techniques are widely applicable to a variety of acoustic and vibration problems.

A. Basic Principles

The basic broad-band ANC system shown in Fig. 1 is described in an adaptive system identification framework illustrated in Fig. 2, in which an adaptive filter $W(z)$ is used to estimate an unknown plant $P(z)$. The primary path $P(z)$ consists of the acoustic response from the reference sensor to the error sensor where the noise attenuation is to be realized. If the plant is dynamic, the adaptive algorithm then has the task of continuously tracking time variations of the plant dynamics. The most important difference between Fig. 2 and the traditional system identification scheme is the use of an acoustic summing junction instead of the subtraction of electrical signals. However, for consistency

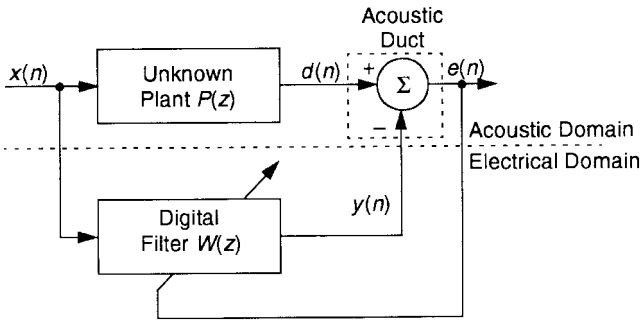

Fig. 2. System identification viewpoint of ANC.

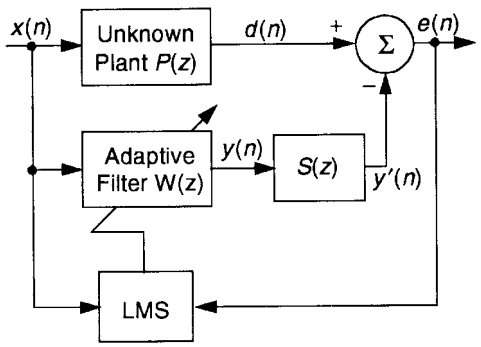

Fig. 3. Simplified block diagram of ANC system.

we will continue to represent the summing junction by a subtraction; it is really arbitrary anyway because it can be implemented with a sign change of the secondary signal [4].

The objective of the adaptive filter $W(z)$ is to minimize the residual error signal $e(n)$. From Fig. 2, $E(z) = 0$ after the adaptive filter $W(z)$ converges. We then have $W(z) = P(z)$ for $X(z) \neq 0$, which implies that $y(n) = d(n)$. Therefore, the adaptive filter output $y(n)$ is identical to the primary disturbance $d(n)$. When $d(n)$ and $y(n)$ are acoustically combined, the residual error is $e(n) = d(n) - y(n) = 0$, which results in perfect cancellation of both sounds based on the principle of superposition.

The performance of ANC can be determined by frequency-domain analysis of the residual error signal $e(n)$. The autopower spectrum of $e(n)$ is given by [4]

$$S_{ee}(\omega) = [1 - C_{dx}(\omega)]S_{dd}(\omega) \tag{1}$$

where $C_{dx}(\omega)$ is the magnitude-squared coherence function [28] between two wide-sense stationary random processes $d(n)$ and $x(n)$ and $S_{dd}(\omega)$ is the autopower spectrum of $d(n)$. This equation indicates that the performance of the ANC system is dependent on the coherence, which is a measure of noise and the relative linearity of the two processes $d(n)$ and $x(n)$. In order to realize a small residual error, it is necessary to have very high coherence [$C_{dx}(\omega) \approx 1$] at frequencies for which there is significant disturbance energy. The maximum noise reduction of an ANC system at frequency ω in decibels is given by $-10\log_{10}[1-C_{dx}(\omega)]$.

As illustrated in Fig. 1, after the reference signal is picked up by the reference sensor, the controller will have some time to calculate the right output to the canceling loudspeaker. If this electrical delay becomes longer than the acoustic delay from the reference microphone to the canceling loudspeaker, the performance of the system will be substantially degraded. That is because the controller response is noncausal when the electrical delay is longer than the acoustic delay. When the causality condition is met, the ANC system is capable of canceling broad-band random noise. Note that if causality is not possible, the system can effectively control only narrow-band or periodic noise.

B. Secondary-Path Effects

The use of the adaptive filter for ANC application shown in Fig. 1 is complicated by the fact that the summing junction in Fig. 2 represents acoustic superposition in the space from the canceling loudspeaker to the error microphone, where the primary noise is combined with the output of the adaptive filter. Therefore, it is necessary to compensate for the secondary-path transfer function $S(z)$ from $y(n)$ to $e(n)$, which includes the digital-to-analog (D/A) converter, reconstruction filter, power amplifier, loudspeaker, acoustic path from loudspeaker to error microphone, error microphone, preamplifier, antialiasing filter, and analog-to-digital (A/D) converter. For purposes of analysis, we shall represent the actual system in Fig. 2 by the block diagram of Fig. 3.

From Fig. 3, the z-transform of the error signal is

$$E(z) = [P(z) - S(z)W(z)]X(z). \tag{2}$$

As discussed with respect to (1), the residual error is limited by the coherence of the reference signal. However, for purposes gaining insight, we shall make the simplifying assumption here that after convergence of the adaptive filter, the residual error is ideally zero [i.e., $E(z) = 0$]. This requires $W(z)$ to realize the optimal transfer function

$$W^{o}(z) = \frac{P(z)}{S(z)}. \tag{3}$$

In other words, the adaptive filter $W(z)$ has to simultaneously model $P(z)$ and inversely model $S(z)$. A key advantage of this approach is that with a proper model of the plant, the system can respond instantaneously to changes in the input signal caused by changes in the noise sources. However, the performance of an ANC system depends largely upon the transfer function of the secondary path. By introducing an equalizer, a more uniform secondary path frequency response is achieved. In this way, the amount of noise reduction can often be increased significantly [29]. In addition, a sufficiently high-order adaptive FIR filter is required to approximate a rational function $1/S(z)$ shown in (3). It is impossible to compensate for the inherent delay due to $S(z)$ if the primary path $P(z)$ does not contain a delay of at least equal length.

C. Filtered-X LMS Algorithm

The introduction of the secondary-path transfer function into a controller using the standard LMS algorithm shown in Fig. 3 will generally cause instability [30]. This is because the error signal is not correctly "aligned" in time with

the reference signal, due to the presence of $S(z)$. There are a number of possible schemes that can be used to compensate for the effect of $S(z)$. Morgan [31] suggested two approaches to solving this problem. The first solution is to place an inverse filter, $1/S(z)$, in series with $S(z)$ to remove its effect. The second solution is to place an identical filter in the reference signal path to the weight update of the LMS algorithm, which realizes the so-called filtered-X LMS (FXLMS) algorithm [9]. Since an inverse does not necessarily exist for $S(z)$, the FXLMS algorithm is generally the most effective approach. The FXLMS algorithm was independently derived by Widrow [32] in the context of adaptive control and Burgess [17] for ANC applications.

1) Derivation of the FXLMS Algorithm: The placement of the secondary-path transfer function following the digital filter $W(z)$ controlled by the LMS algorithm is shown in Fig. 3. The residual signal is expressed as

$$e(n) = d(n) - s(n) * \left[\boldsymbol{w}^T(n)\boldsymbol{x}(n)\right] \tag{4}$$

where n is the time index, $s(n)$ is the impulse response of secondary path $S(z)$, $*$ denotes linear convolution, $\boldsymbol{w}(n) = [w_0(n)\ w_1(n)\cdots w_{L-1}(n)]^T$ and $\boldsymbol{x}(n) = [x(n)\ x(n-1)\cdots x(n-L+1)]^T$ are the coefficient and signal vectors of $W(z)$, respectively, and L is the filter order. The filter $W(z)$ must be of sufficient order to accurately model the response of the physical system.

Assuming a mean square cost function $\xi(n) = E[e^2(n)]$, the adaptive filter minimizes the instantaneous squared error

$$\hat{\xi}(n) = e^2(n) \tag{5}$$

using the steepest descent algorithm, which updates the coefficient vector in the negative gradient direction with step size μ

$$\boldsymbol{w}(n+1) = \boldsymbol{w}(n) - \frac{\mu}{2}\nabla\hat{\xi}(n) \tag{6}$$

where $\nabla\hat{\xi}(n)$ is an instantaneous estimate of the mean-square-error (MSE) gradient at time n and is expressed as $\nabla\hat{\xi}(n) = \nabla e^2(n) = 2[\nabla e(n)]e(n)$. From (4), we have $\nabla e(n) = -s(n) * \boldsymbol{x}(n) = -\boldsymbol{x}'(n)$, where $\boldsymbol{x}'(n) = [x'(n)\ x'(n-1)\cdots x'(n-L+1)]^T$ and $x'(n) = s(n)*x(n)$. Therefore, the gradient estimate becomes

$$\nabla\hat{\xi}(n) = -2\boldsymbol{x}'(n)e(n). \tag{7}$$

Substituting (7) into (6), we have the FXLMS algorithm

$$\boldsymbol{w}(n+1) = \boldsymbol{w}(n) + \mu\boldsymbol{x}'(n)e(n). \tag{8}$$

In practical ANC applications, $S(z)$ is unknown and must be estimated by an additional filter $\hat{S}(z)$. Therefore, the filtered reference signal is generated by passing the reference signal through this estimate of the secondary path

$$\boldsymbol{x}'(n) = \hat{s}(n) * \boldsymbol{x}(n) \tag{9}$$

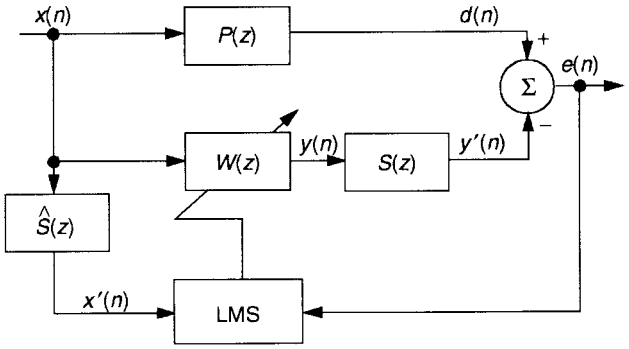

Fig. 4. Block diagram of ANC system using the FXLMS algorithm.

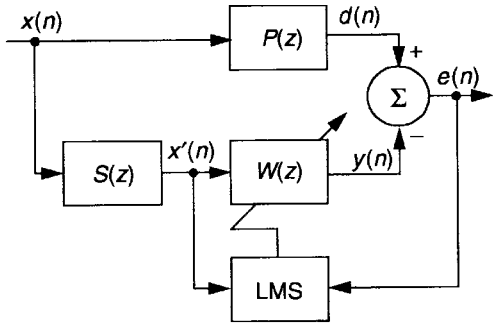

Fig. 5. Equivalent diagram of Fig. 4 for slow adaptation and $\hat{S}(z) = S(z)$.

where $\hat{s}(n)$ is the estimated impulse response of the secondary-path filter $\hat{S}(z)$. The block diagram of ANC system using the FXLMS algorithm is illustrated in Fig. 4.

The FXLMS algorithm appears to be very tolerant of errors made in the estimation of $S(z)$ by the filter $\hat{S}(z)$. As shown by Morgan [31], within the limit of slow adaptation, the algorithm will converge with nearly 90° of phase error between $\hat{S}(z)$ and $S(z)$. Therefore, offline modeling can be used to estimate $S(z)$ during an initial training stage for most ANC applications. The detailed experimental setup and procedure for offline secondary-path modeling is summarized in [4]. The topic of adaptive online secondary-path modeling will be discussed later in Section VI.

2) Analysis of the FXLMS Algorithm: Consider the case in which the control filter $W(z)$ is changing slowly, so that the order of $W(z)$ and $S(z)$ in Fig. 4 can be commuted [9], [31]. If $\hat{S}(z) = S(z)$, Fig. 4 is then simplified to Fig. 5. Since the output of the adaptive filter now carries through directly to the error signal, the traditional LMS algorithm analysis method can be used, although the relevant reference signal is now $x'(n)$, which is produced by filtering $x(n)$ through $S(z)$. This method gives accurate results if adaptation is slow, that is, if the step size μ is small.

The maximum step size that can be used in the FXLMS algorithm is approximately [33]

$$\mu_{\max} = \frac{1}{P_{x'}(L+\Delta)} \tag{10}$$

where $P_{x'} = E[x'^2(n)]$ is the power of the filtered reference signal $x'(n)$, and Δ is the number of samples corresponding

to the overall delay in the secondary path. Therefore, the delay in the secondary path influences the dynamic response of the ANC system by reducing the maximum step size in the FXLMS algorithm.

Boucher and coworkers [34], [35] discuss the effects of secondary path modeling phase errors on the optimum step size and convergence time. The analysis applies to the special case when the reference signal is narrow-band but the disturbance is still broad band. Numeric results suggest that phase errors of 40° hardly affect the convergence speed of the algorithm. However, convergence will slow appreciably as the phase difference approaches 90° because the poles come closer to the unit circle. For narrow-band signals, errors in the estimation of the secondary path transfer function can be considered in two parts: amplitude errors and phase errors [36]. Any magnitude estimation error will proportionally change the power of $x'(n)$ and hence will simply scale the ideal stability bound accordingly. However, there is no simple relationship between phase modeling error and stability in the range of $\pm 90°$.

Another complication that often arises in the broad-band case is that measurement noises $u(n)$ and $v(n)$ are present in the reference and error signals, respectively. The optimal unconstrained transfer function $W^o(z)$ is [4]

$$W^{o}(z) = \frac{P(z)S_{xx}(z)}{[S_{xx}(z) + S_{uu}(z)]S(z)}. \tag{11}$$

This equation shows that $W^o(z)$ is independent of the measurement noise $v(n)$ associated with the error sensor. However, the measurement noise $u(n)$ associated with the reference sensor does affect the optimum weight and hence reduces the cancellation performance. The best frequency response of the controller is a compromise between cancellation of the primary noise $x(n)$ and amplification of the measurement noise through the controller [25]. Some practical considerations to reduce undesired measurement noise are given in [4].

In Fig. 4, if the secondary-path transfer function $S(z)$ is modeled as a pure delay Δ, then $\hat{S}(z)$ is replaced by a delay Δ. This special case of the FXLMS algorithm is also known as the delayed LMS algorithm [37], [38]. The upper bound for the step size [38] depends on the delay Δ and is in close agreement with Elliott's approximation given in (10). Therefore, efforts should be made to keep the delay small, such as decreasing the distance between the error sensor and the secondary source and reducing the delay in electrical components.

3) Leaky FXLMS Algorithm: In an ANC system, the direct application of the FXLMS algorithm sometimes leads to another problem: high noise levels associated with low-frequency resonances, which may cause nonlinear distortion by overloading the secondary source. An obvious solution to this problem is the introduction of output power constraints. Similar results can be obtained by constraining the adaptive filter weights by modifying the cost function as [39]

$$\hat{\xi}(n) = e^2(n) + \gamma \boldsymbol{w}^T(n)\boldsymbol{w}(n) \tag{12}$$

where γ is a weighting on the control effort. Following the derivation of the FXLMS algorithm, the update algorithm can be derived as

$$\boldsymbol{w}(n+1) = \nu \boldsymbol{w}(n) + \mu \boldsymbol{x}'(n)e(n) \tag{13}$$

where $\nu = 1 - \mu\gamma$ is the leakage factor and $0 < \nu < 1$. This leaky FXLMS algorithm also reduces numeric error in the finite-precision implementation [4], [40]. The introduction of a leakage factor has a considerable stabilizing effect on the adaptive algorithm, especially when very large source strengths are used [39], [41].

As shown in [4], the leakage has the effect of modifying the diagonalized correlation matrix of the input process. All eigenvalues are positive even if some of the original input eigenvalues are zero. This guarantees a unique solution and a bounded time constant for all modes. The price of leakage is increased complexity of the weight update equation and the introduction of a bias into the converged solution [13]. The choice of γ thus represents a compromise between biasing the convergence weight vector away from the optimum solution and moderating the control effort.

D. Feedback Effects and Solutions

The acoustic ANC system shown in Fig. 1 uses a reference microphone to pick up the reference noise and processes this input with an adaptive filter to generate an antisound $y(n)$ to cancel primary noise acoustically in the duct. Unfortunately, the antisound output to the loudspeaker also radiates upstream to the reference microphone, resulting in a corrupted reference signal $x(n)$. The coupling of the acoustic wave from the canceling loudspeaker to the reference microphone is called acoustic feedback. Similar effects take place in vibration ANC systems due to feedback from the control actuator to reference sensor.

A more general block diagram of an ANC system that includes feedback from the secondary source to the reference sensor is shown in Fig. 6, where $u(n)$ is the primary noise, $x(n)$ is the signal picked up by the reference sensor, and $F(z)$ is the feedback path transfer function from the output of adaptive filter $W(z)$ to the reference sensor. The steady-state transfer function of the adaptive filter is [4]

$$W^{o}(z) = \frac{P(z)}{S(z) + P(z)F(z)}. \tag{14}$$

From Fig. 6, the open-loop transfer function associated with the feedback loop is given as $H_{\mathrm{OL}}(z) = W(z)F(z)$. If the adaptive filter $W(z)$ has converged to the noiseless optimal solution (14), then

$$H_{\mathrm{OL}}(z) = \frac{P(z)F(z)}{S(z) + P(z)F(z)}. \tag{15}$$

This open-loop transfer function can be used to test the stability of the system [42]. Instability will occur if the open-loop phase lag reaches 180° while the open-loop gain is greater than unity.

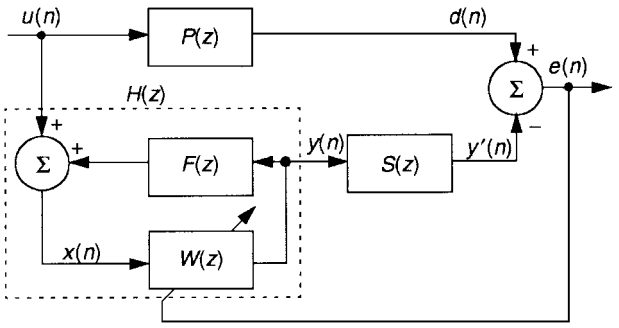

Fig. 6. Block diagram of ANC system with feedback.

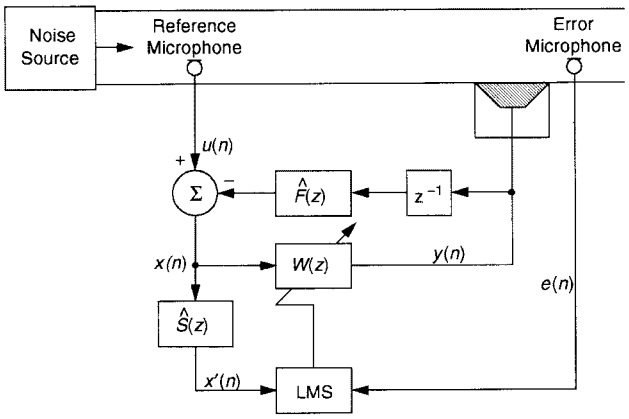

Fig. 7. ANC with acoustic feedback neutralization.

1) Feedback Neutralization: The simplest approach to solving the feedback problem is to use a separate feedback cancellation, or "neutralization," filter within the controller, which is exactly the same technique as used in acoustic echo cancellation [43]. This electrical model of the feedback path is driven by the secondary signal, and its output is subtracted from the reference sensor signal [44]. A duct-acoustic ANC system using the FXLMS algorithm with feedback neutralization is illustrated in Fig. 7. The feedback component of the reference microphone signal is canceled electronically using a feedback neutralization filter $\hat{F}(z)$, which models the feedback path $F(z)$.

Since the primary noise is highly correlated with the antinoise, the adaptation of the feedback neutralization filter must be inhibited when the ANC system is in operation, similar to adaptive echo cancellation during periods of double talk. Thus, feedback neutralization is achieved, in effect, by using an offline adaptive method for determining the transfer function of the feedback path. The models $\hat{S}(z)$ and $\hat{F}(z)$ can be estimated simultaneously by using the offline modeling technique [4].

2) Adaptive IIR Filter: Equation (14) shows that when feedback is present, the optimal solution of the adaptive filter is generally an IIR function with poles and zeros. This rational function can be approximated by an FIR function of sufficient order, but a smaller step size μ then has to be used for stability reasons. The poles of an IIR filter make it possible to obtain well-matched characteristics with a lower order structure, thus requiring fewer arithmetic

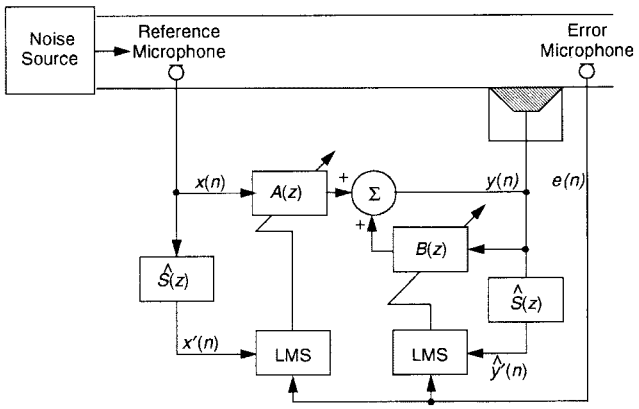

Fig. 8. ANC system using the filtered-U recursive LMS algorithm.

operations [41]. However, the disadvantages of adaptive IIR filters are: 1) IIR filters are not unconditionally stable because of the possibility that some pole(s) of the filter will move outside of the unit circle during the adaptive process, causing instability; 2) the adaptation may converge to a local minimum because the MSE function of adaptive IIR filters is generally nonquadratic; and 3) IIR adaptive algorithms can have a relatively slow convergence rate in comparison with that of FIR filters. A comprehensive discussion of adaptive IIR filters can be found in the literature [45], [46].

A block diagram of an adaptive IIR ANC system [47] is illustrated in Fig. 8. The output signal of the IIR filter $y(n)$ is computed as

$$y(n) = \boldsymbol{a}^T(n)\boldsymbol{x}(n) + \boldsymbol{b}^T(n)\boldsymbol{y}(n-1) \tag{16}$$

where $\boldsymbol{a}(n) \equiv [a_0(n)\ a_1(n) \cdots a_{L-1}(n)]^T$ is the weight vector of $A(z)$, $\boldsymbol{x}(n)$ is the reference signal vector, $\boldsymbol{b}(n) \equiv [b_1(n)\ b_2(n) \cdots b_M(n)]^T$ is the weight vector of $B(z)$, and $\boldsymbol{y}(n-1)$ is the output signal vector delayed by one sample. Many algorithms can be employed to find the optimal set of coefficients a_l and b_m to minimize the error signal $e(n)$. In 1976, Feintuch [48] suggested that the recursion based on the old output gradients is negligible. Based on this suggestion, the "filtered-U recursive LMS algorithm" [49] for ANC is derived as [4]

$$\boldsymbol{a}(n+1) = \boldsymbol{a}(n) + \mu\boldsymbol{x}'(n)e(n) \tag{17}$$

$$\boldsymbol{b}(n+1) = \boldsymbol{b}(n) + \mu\hat{\boldsymbol{y}}'(n-1)e(n) \tag{18}$$

where $\hat{\boldsymbol{y}}'(n-1) = \hat{s}(n) * \boldsymbol{y}(n-1)$ is the filtered version of the canceling signal vector at time $n-1$. In practice, it is reasonable to use a higher order for $B(z)$ than for $A(z)$ [50]. Real-time experiments have been conducted to test the system performance for various reference microphone locations, error microphone locations, and different time-varying sources, such as a centrifugal fan and diesel engine [51].

Given the complexities associated with the pole-zero structure of $P(z), S(z)$, and $F(z)$, one cannot predict the values to which $A(z)$ and $B(z)$ will converge. Also, global convergence and stability of the filtered-U recursive LMS

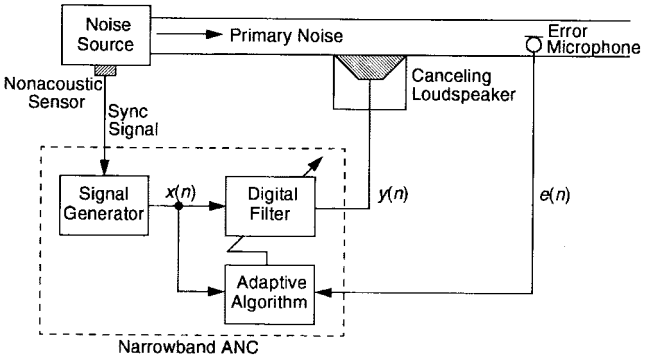

Fig. 9. Basic configuration of narrow-band ANC system.

algorithm have never been proven formally. A modified leaky version of the simplified hyperstable adaptive recursive filter (SHARF) algorithm [52] has been developed for ANC applications to improve the stability of the IIR adaptive filter [53]. In that algorithm, a lowpass filter is used to smooth the error signal for the filtered-U recursive LMS algorithm, thereby providing a higher stability margin.

III. Narrowband Feedforward ANC

Many noises are periodic, such as those generated by engines, compressors, motors, fans, and propellers. Direct observation of the mechanical motion of such sources generally is possible by using an appropriate sensor, which provides an electrical reference signal that contains the fundamental frequency and all the harmonics of the primary noise. However, this technique is only effective for periodic noise because the fundamental driving frequency is the only reference information available.

A. Introduction

A basic block diagram of narrow-band ANC for reducing periodic acoustic noise in a duct is illustrated in Fig. 9. This system controls harmonic sources by adaptively filtering a synthesized reference signal $x(n)$ internally generated by the ANC system. This technique has the following advantages: 1) undesired acoustic feedback from the canceling loudspeaker back to the reference microphone is avoided; 2) nonlinearities and aging problems associated with the reference microphone are avoided; 3) the periodicity of the noise removes the causality constraint; 4) the use of an internally generated reference signal results in the ability to control each harmonic independently; and 5) it is only necessary to model the acoustic plant transfer function over frequencies in the vicinity of the harmonic tones; thus, an FIR filter with substantially lower order may be used.

The reference signal generator is triggered by a synchronization pulse from a nonacoustic sensor, such as a tachometer signal from an automotive engine. In general, two types of reference signals are commonly used in narrow-band ANC systems: 1) an impulse train with a period equal to the inverse of the fundamental frequency of the periodic noise [54] and 2) sinewaves that have the same frequencies as the corresponding harmonic tones to be canceled. The first technique is called the waveform synthesis method, which was proposed by Chaplin [55]. The second technique embodies the adaptive notch filter, which was originally developed for the cancellation of tonal interference [56] and applied to periodic ANC [57].

The waveform synthesis method discussed next in Section III-B employs synchronous sampling. However, for some applications, the actual period will vary from the nominal value as a function of loading conditions. Therefore, it is sometimes desirable to operate asynchronously with a fixed sampling rate so that the secondary-path estimate filter coefficients do not have to be changed as a function of actual machine rotation rate. Also, some digital signal processors cannot be efficiently utilized on a synchronous signal-driven basis. Asynchronous ANC systems using the FXLMS algorithm eliminate the problem of having to change $\hat{S}(z)$ as the sampling rate varies and are implicit in the later formulations of Sections III-C and III-D.

B. Waveform Synthesis Method

1) Structures and Algorithms: The waveform synthesizer [55] stores canceling noise waveform samples $\{w_l(n), l = 0, 1, \ldots, L-1\}$ in unique contiguous memory addresses, where L is the number of samples over one cycle of the waveform and n is the current time index. These samples represent the required waveform to be generated and are sequentially sent to a D/A converter to produce the actual canceling noise waveform for the secondary loudspeaker. Thus

$$y(n) = w_{j(n)}(n) \tag{19}$$

represents the $j(n)$th element of waveform samples, where $j(n) \equiv n \bmod L$ and can be implemented as a pointer incremented in a circular fashion between zero and $L-1$ for each sampling period, controlled by interrupts generated from the synchronization signal.

The residual noise picked up by the error microphone is synchronously sampled with the reference signal timing pulses. In a practical system, there is a delay between the time the signal $[y(n) = w_{j(n)}(n)]$ is fed to the loudspeaker and the time it is received at the error microphone. This delay can be accommodated by subtracting a time offset from the circular pointer $j(n)$. Thus, the adaptation unit adjusts the values of the waveform samples using a variant of the LMS algorithm

$$w_l(n+1) = \begin{cases} w_l(n) + \mu e(n), & l = j(n-\Delta) \\ w_l(n), & \text{otherwise} \end{cases} \tag{20}$$

where $\Delta = \lfloor \tau/T \rfloor$ and τ is the time delay, which is constant for a given loudspeaker-microphone arrangement, T is the sampling period, and $\lfloor x \rfloor$ = greatest integer less than or equal to x. This offset number Δ must be updated as the sampling rate varies, since it is synchronized with the noise source.

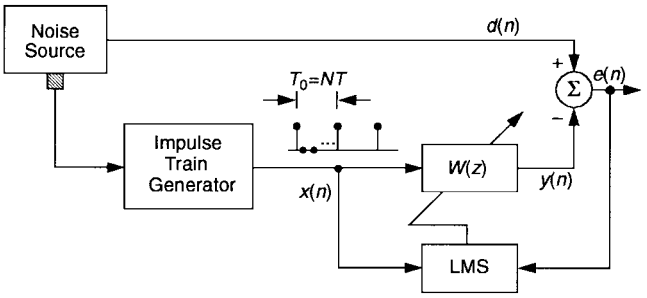

Fig. 10. Equivalent diagram of waveform synthesis method using impulse train input and neglecting secondary path effects.

2) Principle and Analysis: The waveform synthesis method is equivalent to an adaptive FIR filter of order $L = N$ excited by a Kronecker impulse train of period $N = T_0/T$ samples [4]

$$x(n) = \sum_{k=-\infty}^{\infty} \delta(n - kN) \tag{21}$$

where $\delta(\cdot)$ is the discrete Kronecker delta function and $T_0 = 2\pi/\omega_0$ is the period of the noise with fundamental angular frequency ω_0. Temporarily neglecting secondary path effects, Fig. 10 shows how the periodic noise is canceled by the output of an adaptive filter using the periodic impulse train as the reference input $x(n)$.

For reference signal (21) and an adaptive filter with order $L = N$, the transfer function $H(z)$ between the primary input $D(z)$ and the error output $E(z)$ is derived as [54]

$$H(z) = \frac{E(z)}{D(z)} = \frac{1 - z^{-L}}{1 - (1 - \mu)z^{-L}}. \tag{22}$$

The zeros have constant amplitude ($|z| = 1$) and are equally spaced ($2\pi/L$) on the unit circle of the z plane to create nulls in the frequency response at harmonic frequencies $k\omega_0$. Therefore, the tonal components of the periodic noise at the fundamental and harmonic frequencies are attenuated by this multiple-notch filter. The poles have the same frequency as the zeros but are equally spaced on a circle at distance $(1 - \mu)$ from the origin. The effect of the poles is to introduce a resonance in the vicinity of the null, thus reducing the bandwidth of the notch.

Equation (22) also gives a practical limitation on the value of μ from stability considerations; that is, $0 < \mu < 1$ for an impulse train of unit amplitude. The 3-dB bandwidth of each notch for $\mu \ll 1$ is approximated as $B \approx \mu/\pi T$ (Hz) [54]. This shows that the bandwidth of the notch filter is proportional to the step size μ. In the general case, the time constant of the response envelope decay is approximately $\tau \approx T/\mu$ (second). Therefore, there is tradeoff between the notch bandwidth and the duration of the transient response, which is determined by the step size and the sampling rate of the narrow-band ANC system.

3) FXLMS Algorithm: As discussed in Section II, the effects of the secondary path $S(z)$ must be compensated for by using the FXLMS algorithm. Assuming a secondary-path estimate $\hat{S}(z)$ of order $L = N$, the output of $\hat{S}(z)$ is computed as

$$x'(n) = \sum_{l=0}^{L-1} \hat{s}_l x(n - l) = \hat{s}_{j(n)} \tag{23}$$

where $\hat{s}_l$ is the lth coefficient of the filter $\hat{S}(z), j(n) = n \bmod L$ is the same circular pointer as that used in (19). Therefore, the FXLMS algorithm for synchronous waveform synthesis ANC systems becomes [4]

$$w_l(n + 1) = w_l(n) + \mu e(n)\hat{s}_{k(n,l)}, \quad l = 0, 1, \ldots, L - 1 \tag{24}$$

where $k(n, l) \equiv (n - l) \bmod L$.

The transfer function of the synchronous periodic controller in the ideal environment [without $S(z)$] is specified by (22). The presence of $S(z)$ modifies the transfer function of the controller to [58]

$$H(z) = \frac{1 - z^{-L}}{1 - [1 - \mu S(z)]z^{-L}}. \tag{25}$$

The detailed dynamic stability limits are analyzed elsewhere [58].

4) Delayed LMS Algorithm: If the case of a single sinusoid is considered, then the steady-state response of the secondary path can be modeled by a pure delay. Therefore, the compensator can be approximated as $\hat{S}(z) = z^{-\Delta}$, where Δ is the number of samples of delay from $y(n)$ to $e(n)$. If the delay value Δ is small compared to the filter length L, the convergence behavior of the delayed LMS algorithm is not significantly impaired from that of the conventional LMS algorithm [37]–[39].

The steady-state transfer function $H(z)$ from $D(z)$ to $E(z)$ for the delayed LMS algorithm is [59]

$$H(z) = \frac{1 - z^{-L}}{1 - \left(1 - \mu z^{-\lfloor \Delta/L \rfloor L}\right) z^{-L}}. \tag{26}$$

This transfer function shows that the delayed coefficient adaptation changes the pole structure. In addition to reducing the bandwidth of the notch, the inclusion of delay shifts the angle of the poles away from $k\omega_0$, and accordingly increases the out-of-band overshoot of the frequency response [59], [60]. As the step size μ and/or the delay in the secondary path is increased, these out-of-band peaks become larger until the system finally becomes unstable.

C. Adaptive Notch Filters

1) Narrow-Band Adaptive Noise Canceler: An adaptive notch filter can be realized by using an adaptive noise canceler [56] with a sinusoidal reference signal. The advantages of the adaptive notch filter are that it offers easy control of bandwidth, an infinite null, and the capability to adaptively track the exact frequency of the interference. A single-frequency adaptive noise canceler with two adaptive weights is illustrated in Fig. 11. The reference input is a cosine wave $x(n) = x_0(n) = A\cos(\omega_0 n)$, where A and ω_0 are the amplitude and frequency, respectively, of the

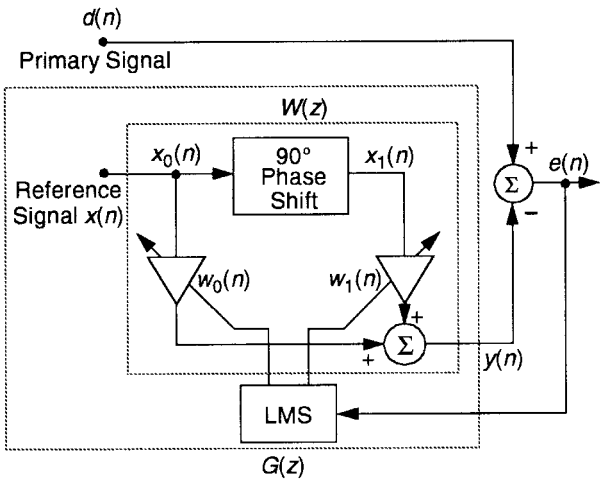

Fig. 11. Single-frequency adaptive notch filter.

reference signal. A 90° phase shifter is used to produce the quadrature reference signal $x_1(n) = A\sin(\omega_0 n)$.

The steady-state transfer function $H(z)$ from the primary input $d(n)$ to the noise canceler output $e(n)$ is [56]

$$H(z) = \frac{E(z)}{D(z)} = \frac{z^2 - 2z\cos\omega_0 + 1}{z^2 - (2-\mu A^2)z\cos\omega_0 + 1 - \mu A^2}. \tag{27}$$

The zeros of $H(z)$ are located in the z plane at $z = e^{\pm j\omega_0}$, being precisely on the unit circle at angle ω_0. The adaptive noise canceler therefore acts as a tunable notch filter, with a notch located at the reference frequency ω_0. For a general Lth order adaptive filter, (27) becomes [61]

$$H(z) = \frac{z^2 - 2z\cos\omega_0 + 1}{z^2 - \left(2 - \dfrac{\mu L A^2}{2}\right)z\cos\omega_0 + 1 - \dfrac{\mu L A^2}{2}}. \tag{28}$$

Therefore, the poles are dependent on the number of taps L, and that will affect the shape of the notch.

The sharpness of the notch is determined by the closeness of the poles to the zeros. The 3-dB bandwidth of the notch filter is estimated as [61]

$$B \approx \frac{\mu L A^2}{4\pi T} \quad \text{(Hz)}. \tag{29}$$

When the interfering sinusoid frequency changes rapidly or jitters around, the notch width must cover a wider frequency range. This can be accomplished by using a larger μ, which has the effect of providing faster tracking and of producing a wider notch. For $L = 2$, the system has very fast convergence and the $1/e$ time constant of the adaptation is approximated as [4]

$$\tau_{\text{mse}} \leq \frac{2T}{\mu A^2} \quad \text{(s)} \tag{30}$$

which is determined by the power of the reference sinewave and the step size μ.

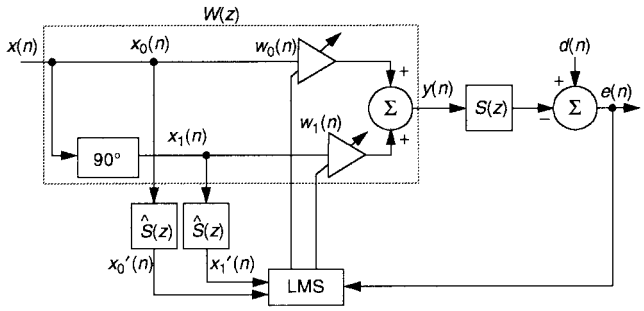

Fig. 12. Single-frequency ANC system using the FXLMS algorithm.

2) Single-Frequency ANC: The application of the adaptive notch filter to periodic ANC has been developed by Ziegler [57]. A recursive quadratic oscillator provides two orthogonal components $x_0(n)$ and $x_1(n)$, which are used as reference inputs for the adaptive filter. These two signals are separately weighted and then summed to produce the canceling signal $y(n)$. The delayed LMS algorithm updates the filter weights to minimize the residual error $e(n)$. Thus

$$w_l(n+1) = w_l(n) + \mu e(n) x_l(n-\Delta), \qquad l = 0,1 \tag{31}$$

where Δ is used to compensate for the secondary-path transfer function.

Alternatively, the above delay unit can be replaced by a secondary-path estimate $\hat{S}(z)$ as in the FXLMS algorithm illustrated in Fig. 12. The adaptive weights are updated as

$$w_l(n+1) = w_l(n) + \mu x_l'(n) e(n), \qquad l = 0,1 \tag{32}$$

where $x_0'(n)$ and $x_1'(n)$ are the filtered versions of $x_0(n)$ and $x_1(n)$, respectively, obtained through the secondary-path estimate $\hat{S}(z)$.

In the limit of slow adaptation, the transfer function of the narrow-band ANC system then becomes [4]

$$H(z) = \frac{z^2 - 2z\cos\omega_0 + 1}{z^2 - [2\cos\omega_0 - \beta\cos(\omega_0 - \phi_\Delta)]z + 1 - \beta\cos\phi_\Delta} \tag{33}$$

where $\beta = \mu A^2 A_s$, A_s is the amplitude of $S(z)$ at frequency ω_0, and $\phi_\Delta = \phi_s - \phi_{\hat{s}}$ is the phase difference between $S(z)$ and $\hat{S}(z)$ at ω_0. For small $\beta, H(z)$ has complex conjugate poles at radius $r_{\text{p}} = \sqrt{1 - \beta\cos\phi_\Delta}$. Since all the terms composing β are positive, the radius of the pole can be greater than one only if $\cos\phi_\Delta$ is negative. Accordingly, the stability condition is

$$\cos\phi_\Delta > 0 \quad \text{or} \quad -90° < \phi_\Delta < 90° \tag{34}$$

and the convergence time constant is slowed down by a factor of $1/\cos\phi_\Delta$ [31].

Another method for analyzing the stability and transient response of the adaptive notch filter using the FXLMS algorithm is to formulate the problem in the complex weight domain and apply standard control theory [62]. Application of this analysis technique showed that large out-of-band gain can lead to instability. One solution to

the out-of-band gain problem is to equalize the secondary-path transfer function $S(z)$ in phase and amplitude over the entire band. An alternative solution is to control the out-of-band response by either employing a bandpass filter in the secondary path before demodulation or a lowpass filter after demodulation [62]. However, there is an inherent tradeoff here because in addition to attenuating out-of-band gain, a bandpass filter will also introduce delay. Another solution consists of two interconnected adaptive filters using the same internally generated reference signal [63].

3) Simplified Single-Frequency ANC: Ziegler's technique requires either two tables (cosine and sine) in the waveform generator to generate $x_0(n)$ and $x_1(n)$ or uses only one cosine table and a 90° phase shift unit to generate the sine waveform. In a simplified single-frequency ANC system [64], a single-cosine-wave generator is used to generate a reference input $x(n)$, which is then fed to a simple second-order FIR filter, where both weights are updated by the FXLMS algorithm. (See [4] for details.) In this case, the fastest convergence can be achieved by choosing a sampling rate equal to four times the frequency of the sinewave.

D. Multiple-Frequency ANC

In practical applications, periodic noise usually contains multiple tones at the fundamental frequency and at several harmonic frequencies. This type of noise can be attenuated by a filter with multiple notches. In general, realization of multiple notches requires higher order filters, which can be implemented by direct, parallel, direct/parallel, or cascade forms.

1) Direct Form: A method for eliminating multiple sinusoidals or other periodic interference was proposed by Glover [61]. The reference input is a sum of M sinusoids

$$x(n) = \sum_{m=1}^{M} A_m \cos(\omega_m n) \tag{35}$$

where A_m and ω_m are, respectively, the amplitude and the frequency of the mth sinusoid. When the frequencies of the reference sinusoids are close together, a long filter $(L \gg 2M)$ is required to give good resolution between adjacent frequencies. This is an undesired solution since a higher order adaptive LMS filter results in slower convergence, higher excess MSE, and higher numeric errors. An application of Glover's method for actively attenuating engine-generated noise has been proposed [65].

2) Parallel Form: For the case in which the undesired primary noise contains M sinusoids, M two-weight adaptive filters can be connected in parallel to attenuate these narrow-band components. The canceling signal is a sum of M adaptive filter outputs

$$y(n) = \sum_{m=1}^{M} y_m(n) \tag{36}$$

where each output $y_m(n)$ is derived as in the single-frequency case. Since only one error sensor is used, there is only one error signal $e(n)$, which is used to update all M adaptive filters based on the FXLMS algorithm.

3) Direct/Parallel Form: A configuration of multiple reference signal generators and corresponding adaptive filters has been developed [66] to improve the performance of ANC systems for automotive applications. The idea is to separate a collection of many harmonically related sinusoids into mutually exclusive sets that individually have frequencies spaced out as far as possible. In general, if there are M harmonics to be canceled and K $(K<M)$ signal generators are used, each reference signal $x_k(n), k = 1,2,\ldots,K$ contains staggered sinusoidal frequencies of every other Kth harmonic. These reference signals are processed by their corresponding adaptive filters. By partitioning signal component frequencies in this fashion, the accuracy and rate of convergence of each adaptive filter can be significantly improved. This is because the frequency difference between any two successive sinusoidal components in $x_k(n)$ is effectively increased, as compared to the direct implementation technique.

4) Cascade Form: Ideally, multiple-sinusoid references are more effectively employed in a cascade of M second-order single-frequency notch filters. The overall response of such an arrangement is given by [60]

$$H(z) = \prod_{m=1}^{M} H_m(z) = \prod_{m=1}^{M} \frac{1}{1 + S(z)W_m(z)} \tag{37}$$

where $W_m(z)$ is the mth section adaptive filter. Each $W_m(z)$ produces a pole at frequency ω_m, and so each $H_m(z)$ produces a notch at ω_m. If an estimate of the secondary-path transfer function is available, it is possible to configure a "pseudocascade" arrangement [60] that ideally performs as a true cascade but requires only one secondary path estimate $\hat{S}(z)$. The pseudocascade FXLMS notch filters are expandable to any number of stages and can theoretically cover an arbitrarily wide bandwidth.

5) Rectangular-Wave Reference Signal: The rectangular-wave $x(t)$ potentially contains the fundamental and all harmonic components of the periodic noise. The shape of the spectrum of $x(t)$ is dependent on the duty-cycle ratio τ/T_0, where τ and T_0 are the pulse width and the fundamental period of the rectangular wave. (See [4], [67], and [68] for details.)

E. Active Noise Equalizers

The design of an ANC system usually pursues maximal attenuation of the incoming noise. However, in some applications, it is desirable to retain a small residual error with specified spectral shape. For example, in a car, truck, or earth-moving machine, the driver needs some audible information about engine speed to be able to control the vehicle safely. The equalization system is called an active noise equalizer [69] and is implemented in the frequency domain [70]. The principle of narrow-band active noise equalization also applies to broad-band noise [71].

A block diagram of the general narrow-band active noise equalizer system for controlling periodic noise is shown in Fig. 13. The output of the two-weight filter, $y(n)$, is split into two branches, the canceling branch

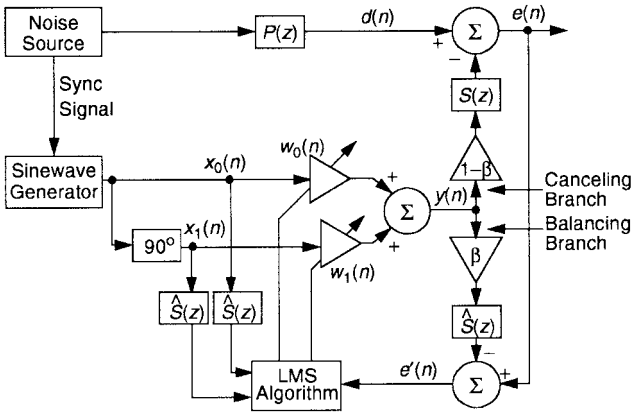

Fig. 13. Block diagram of single-frequency active noise equalizer.

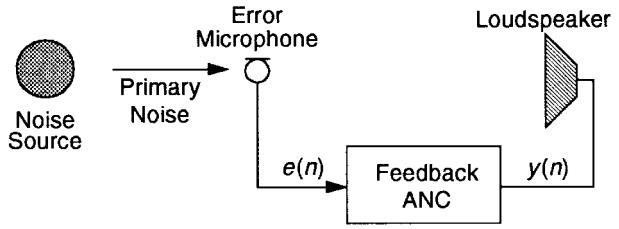

Fig. 14. Single-channel feedback ANC system.

and the balancing branch. The gains β and $(1-\beta)$ are inserted in these two branches to enable adjustment of the residual noise. If the secondary-path estimate is perfect [i.e., $\hat{S}(z) = S(z)$], the pseudo-error $e'(n)$ can be expressed as $e'(n) = d(n) - y(n)$, which is the residual noise of the conventional ANC system. The adaptive filter minimizes the pseudoerror signal using the FXLMS algorithm. After the filter has converged, $e'(n) \approx 0$, the system output is $e(n) = d(n) - (1-\beta)y(n) \approx \beta d(n)$. Thus, the system output $e(n)$ contains a residual component of the narrowband noise whose amplitude is continuously, linearly, and totally controlled by adjusting the gain value β [4], [69].

IV. Feedback ANC

A block diagram for a single-channel feedback ANC system is presented in Fig. 14. The error sensor output is processed by an ANC system to generate the secondary signal. Several nonadaptive feedback ANC systems have been described [3]. In this section, adaptive feedback ANC systems are presented.

A. Adaptive Feedback ANC Systems

A single-channel adaptive feedback ANC system was proposed in [72] and extended to the multiple-channel case in [73]. We view this technique as an adaptive feedforward system that, in effect, synthesizes, or regenerates, its own reference signal, based only on the adaptive filter output and error signal.

1) Structure and Algorithm: The basic idea of an adaptive feedback ANC is to estimate the primary noise and use it as a reference signal $x(n)$ for the ANC filter. In

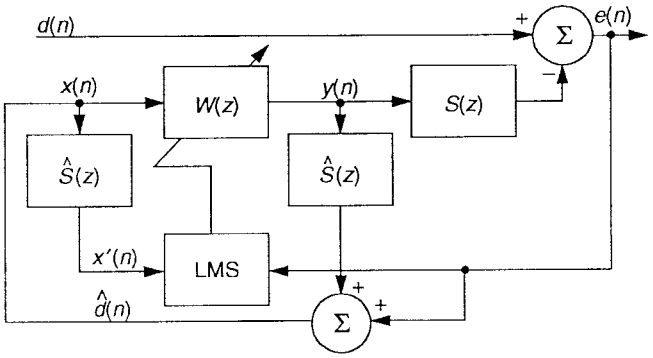

Fig. 15. Wideband adaptive feedback ANC system using the FXLMS algorithm.

Fig. 14, the primary noise is expressed in the z-domain as $D(z) = E(z) + S(z)Y(z)$, where $E(z)$ is the signal obtained from the error sensor and $Y(z)$ is the secondary signal generated by the adaptive filter. If $\hat{S}(z) \approx S(z)$, we can estimate the primary noise $d(n)$ and use this as a synthesized reference signal $x(n)$. That is

$$X(z) \equiv \hat{D}(z) = E(z) + \hat{S}(z)Y(z). \tag{38}$$

This is the reference signal synthesis (regeneration) technique, whereby the secondary signal $y(n)$ is filtered by the secondary-path estimate $\hat{S}(z)$ and then combined with $e(n)$ to regenerate the primary noise.

The complete single-channel adaptive feedback ANC system using the FXLMS algorithm is illustrated in Fig. 15, where $\hat{S}(z)$ is also required to compensate for the secondary path. The reference signal $x(n)$ is synthesized as

$$x(n) \equiv \hat{d}(n) = e(n) + \sum_{m=0}^{M-1} \hat{s}_m y(n-m) \tag{39}$$

where $\hat{s}_m, m = 0, 1, \ldots, M-1$ are the coefficients of the Mth order FIR filter $\hat{S}(z)$ used to estimate the secondary path.

2) Algorithm Analysis: From Fig. 15, we have $x(n) = d(n)$ if $\hat{S}(z) = S(z)$. If the step size μ of the LMS algorithm is small (slow convergence), the adaptive filter $W(z)$ can be commuted with $S(z)$ [9]. If we further assume that the secondary path $S(z)$ can be modeled by a pure delay, that is, $S(z) = z^{-\Delta}$, Fig. 15 is identical to the standard adaptive prediction scheme shown Fig. 16 [74]. The system response from $d(n)$ to $e(n)$ is called the prediction error filter $H(z)$. The adaptive filter $W(z)$ acts as an adaptive predictor of the primary noise $d(n)$ to minimize the residual noise $e(n)$, so the performance of the adaptive feedback ANC system depends on the predictability of the primary noise $d(n)$.

If $\hat{S}(z) = S(z)$, the overall transfer function $H(z)$ of feedback ANC from $d(n)$ to $e(n)$ is [4]

$$H(z) = \frac{E(z)}{D(z)} = 1 - S(z)W(z). \tag{40}$$

Thus, under ideal conditions, the adaptive feedback ANC system shown in Fig. 15 is equivalent to the feedforward

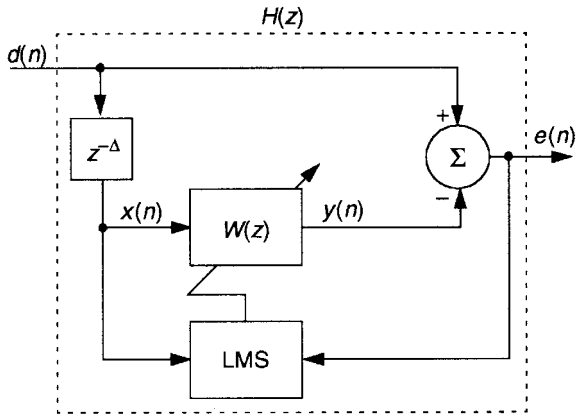

Fig. 16. Block diagram of adaptive predictor.

ANC system discussed in Section II. The stability robustness of the adaptive feedback controller to changes in the plant response can be separately assessed using a generalization of the complementary sensitivity function [75]. The stability robustness is improved by incorporating various forms of effort weighting into the cost function, resulting in the leaky FXLMS algorithm used in feedforward ANC systems.

3) Other Feedback ANC Algorithms: The output-whitening feedback ANC method [76] assumes that the primary noise $d(n)$ is formed by passing white noise through a moving-average (MA) filter $P(z)$. The secondary source is assumed to be placed close enough to the primary source so that the secondary-path transfer function $S(z)$ is minimum phase. Then, from linear estimation theory, the optimal controller is expressed as

$$W^{o}(z) = \frac{\hat{P}(z) - 1}{\hat{S}(z)}. \tag{41}$$

This optimal filter will result in a minimum error signal $e(n)$ that is spectrally white; in other words, all the energy that is predictable from the MA model $P(z)$ has been removed. (See [4] and [33] for further details.) The output-whitening approach is extensible to multiple-channel feedback ANC by utilizing multiple independent controllers with weighted combining [77].

By a somewhat different approach, we first employ secondary-path neutralization similar to the adaptive feedback ANC concept, but then, instead of using the FXLMS algorithm to adapt $W(z)$, we use an open-loop method to estimate the parameters of the primary source model $P(z)$ and predict the next value of $d(n)$ through the secondary path $S(z)$. Oppenheim and coworkers [78] developed an estimation and prediction method for the special case when the secondary path is a pure delay. They postulate an AR model for $P(z)$ and develop a procedure for estimating its parameters. The prediction part is then formulated using the standard Kalman filter setup.

The performance of the Kalman algorithm was compared with the feedforward ANC algorithm discussed in Section II by Zangi [79]. The output of the error sensor contains much more information about the future values

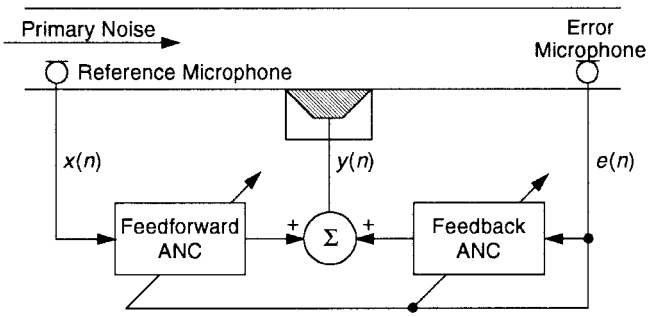

Fig. 17. Hybrid ANC system with combination of feedback ANC and feedforward ANC.

of the primary noise at the error sensor than the output of the reference sensor, which is located away from the control point. This is particularly true whenever the noise field is isotropic and the reference sensor is no longer fully coherent with the noise at the error sensor location.

B. Hybrid ANC Systems

The feedforward ANC systems discussed in Section II use two sensors: a reference sensor and an error sensor. The reference sensor measures the primary noise to be canceled while the error sensor monitors the performance of the ANC system. The adaptive feedback ANC system uses only an error sensor and cancels only the predictable noise components of the primary noise. A combination of the feedforward and feedback control structures is called a hybrid ANC system, as illustrated in Fig. 17 [80]. The reference sensor is kept close to the noise source and provides a coherent reference signal for the feedforward ANC system. The error sensor is placed downstream and senses the residual noise, which is used to synthesize the reference signal for the adaptive feedback ANC filter, as well as to adapt the coefficients of both the feedforward and feedback ANC filters. The feedforward ANC attenuates primary noise that is correlated with the reference signal, while the feedback ANC cancels the predictable components of the primary noise that are not observed by the reference sensor.

The hybrid ANC system using the FIR feedforward ANC and the adaptive feedback ANC is illustrated in Fig. 18, where the secondary signal $y(n)$ is generated using the outputs of both the feedforward ANC filter $A(z)$ and the feedback ANC filter $C(z)$. The combined controller $W(z)$ has two reference inputs: $x(n)$ from the reference sensor and $\hat{d}(n)$, the estimated primary signal. Filtered versions of the reference signals $x'(n)$ and $\hat{d}'(n)$ are used to adapt the coefficients of the filters $A(z)$ and $C(z)$, respectively. A similar hybrid ANC system using the adaptive IIR feedforward ANC and the adaptive feedback ANC can be found in [4]. The advantage of hybrid ANC over other ANC systems is that a lower order filter can be used to achieve the same performance. The hybrid systems also clearly demonstrate an advantage over either the simple feedforward ANC or adaptive feedback ANC system alone when there is significant plant noise.

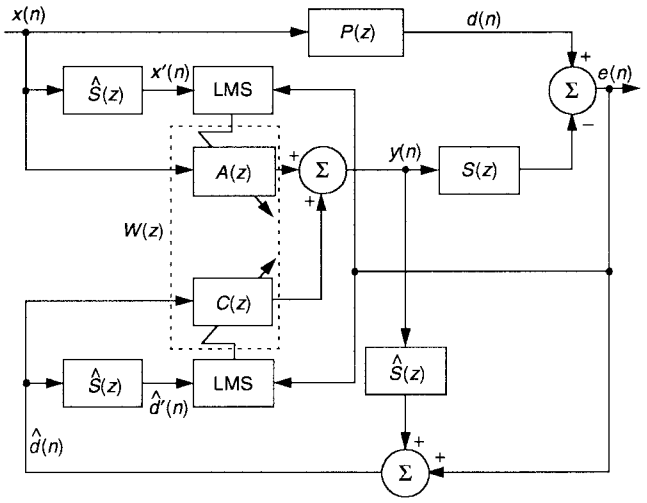

Fig. 18. Hybrid ANC system using the FIR feedforward ANC with the FXLMS algorithm.

V. Multiple-Channel ANC

Since the noise field in an enclosure or a large-dimension duct is more complicated than in a narrow duct, it is generally necessary to use a multiple-channel ANC system with several secondary sources, error sensors, and perhaps even several reference sensors. Some of the best-known applications are the control of exhaust "boom" noise in automobiles [81]–[84], earth-moving machines [85], and the control of propeller-induced noise in flight cabin interiors [86]–[88]. Other ANC applications, such as vibration control in complex mechanical structures, also require multiple channels.

A. Principles

Theoretical predictions, computer simulations, and laboratory experiments on harmonic ANC in a shallow enclosure were presented in a trilogy of papers by Nelson *et al.* [89]–[91]. The total potential acoustic energy $\mathrm{E_p}$ is approximated by the sum of the squares of the outputs of many error sensors distributed throughout the enclosure. This suggests that the multiple-channel ANC system should minimize a cost function

$$\xi = \frac{V}{4\rho c^2 M} \sum_{m=1}^{M} |p_m|^2 \tag{42}$$

where ρ is the density of the acoustic medium, c is the propagation velocity, and p_m is the sound pressure at the mth error sensor position in the enclosure with a total of M error microphones. The significance of (42) is that ξ is a quadratic function, and thus allows the efficient gradient descent method to be employed in the multiple-channel ANC algorithm.

Under low frequency conditions, surprisingly few error sensors are needed to achieve substantial reductions in total noise energy [92]. The location of these error sensors is very important to obtain the best estimate of the total acoustic potential energy. For a rectangular enclosure, a good choice is to put an error sensor in each corner of the enclosure since all modes have a pressure maximum there. The secondary sources should be located in positions where they can couple well to the acoustic modes of the enclosure, or if possible, couple directly to the primary noise source. In the later case, to improve the performance of the system, the distance from the primary to the secondary sources must be less than a quarter-wavelength at the highest frequency [93]. Subtle physical attributes of the multiple-channel ANC system that affect convergence are the placement of the error sensors and the location of the secondary sources [94]. As any two or more channels approach linear dependence at some particular frequency, convergence slows significantly. The remedy for this problem is to move physically or remove one or more of the secondary sources or error sensors.

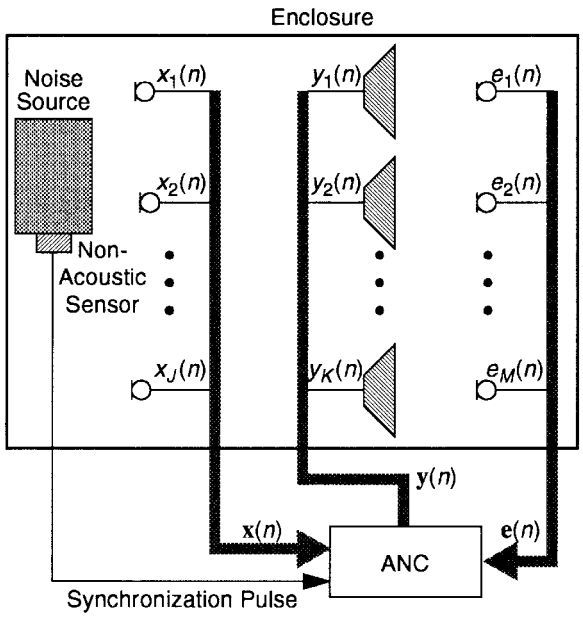

Fig. 19. Structure of a multiple-channel acoustic ANC system with J reference inputs, K secondary sources, and M error sensors.

B. Multiple-Channel FXLMS Algorithms

A multiple-channel acoustic ANC system is illustrated in Fig. 19 as an example of a general multiple-channel ANC system. For narrow-band feedforward multiple-channel ANC systems, a nonacoustic sensor can be used as the reference sensor to generate a reference signal. For broad-band feedforward ANC, the multiple-channel system employs J reference sensors to form the reference signal vector. For adaptive feedback ANC, the reference signals are internally synthesized based on the secondary and error signals. The multiple-channel ANC system generates K canceling signals to drive the corresponding secondary sources, and M error sensors are distributed over desired locations to measure the residual noise components.

A block diagram of a multiple-channel ANC system that includes feedback paths from the secondary sources to the reference sensors is illustrated in Fig. 20. The wide arrows represent an array of signals (acoustic or electrical)

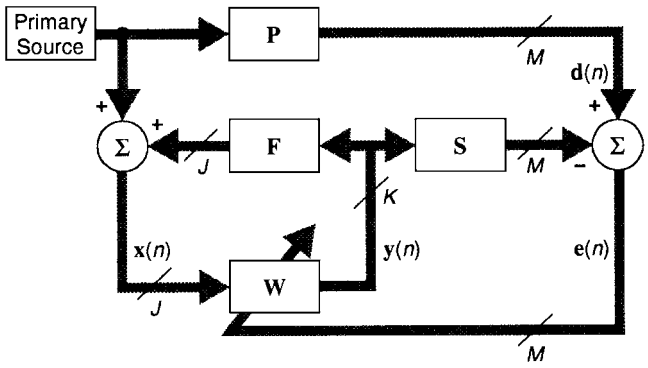

Fig. 20. Block diagram of an adaptive multiple-channel feedforward ANC system with feedback paths.

that are symbolically expressed as vectors. The matrix $\boldsymbol{P}$ represents $M \times J$ primary path transfer functions, $P_{mj}(z)$, from the primary source to each error sensor output $e_m(n)$. The matrix $\boldsymbol{S}$ represents $M \times K$ secondary-path transfer functions, $S_{mk}(z)$, from K secondary sources to M error sensors. Also, the matrix $\boldsymbol{F}$ represents $J \times K$ feedback paths $F_{jk}(z)$ from K secondary sources to J reference sensors. There are $K \times J$ possible feedforward channels, each demanding a separate adaptive filter, and these $K \times J$ adaptive filters are represented by the matrix $\boldsymbol{W}$. A complete set of multiple-channel FXLMS algorithms for broad-band feedforward, narrow-band feedforward, and adaptive feedback ANC systems are introduced in [4].

1) Single-Reference/Multiple-Output Algorithm: The single-reference/multiple-output ANC system aims to control a multidimensional noise field produced by rotating machinery such as engines [39]. As discussed in Section III, a nonacoustic reference sensor is used to avoid feedback. The kth secondary signal $y_k(n)$ is obtained by filtering the reference signal $x(n)$ through the corresponding adaptive FIR filter

$$y_k(n) = \boldsymbol{w}_k^T(n)\boldsymbol{x}(n), \qquad k = 1, 2, \ldots, K \tag{43}$$

where $\boldsymbol{w}_k(n) \equiv [w_{k,0}(n) \;\; w_{k,1}(n) \cdots w_{k,L-1}(n)]^T$ is the weight vector of the kth adaptive filter and $\boldsymbol{x}(n) \equiv [x(n)\, x(n-1) \cdots x(n-L+1)]^T$ is the common reference signal vector for all adaptive filters.

The cost function of the adaptive filters is approximated by the sum of the instantaneous squared errors as

$$\hat{\xi}(n) = \sum_{m=1}^{M} e_m^2(n) = \boldsymbol{e}^T(n)\boldsymbol{e}(n). \tag{44}$$

Following a derivation similar to the single-channel case discussed in Section II, the single-reference/multiple-output FXLMS algorithm is derived and partitioned into K equations [4]

$$\boldsymbol{w}_k(n+1) = \boldsymbol{w}_k(n) + \mu \sum_{m=1}^{M} \boldsymbol{x}'_{km}(n) e_m(n), \qquad k = 1, 2, \ldots, K \tag{45}$$

where

$$\boldsymbol{x}'_{km}(n) \equiv \hat{s}_{mk}(n) * \boldsymbol{x}(n) \tag{46}$$

for $k = 1, 2, \ldots, K$ and $m = 1, 2, \ldots, M$ are the filtered reference signal vectors, which are formed by filtering $\boldsymbol{x}(n)$ by the secondary-path estimates $\hat{S}_{mk}(z)$ from the kth secondary source to the mth error sensor. In (46), $\hat{s}_{mk}(n)$ represents the impulse response of an FIR filter $\hat{S}_{mk}(z)$ that is used to estimate $S_{mk}(z)$. The single-reference/multiple-output FXLMS algorithm is expressed in detail for a $1 \times 2 \times 2$ example in [4]. Similar to the derivation of the leaky FXLMS algorithm given in Section II-C, the cost function (44) can be modified to including a weighting factor. The multiple-channel leaky FXLMS algorithm is similar to (45), except that $\nu \boldsymbol{w}_k(n)$ is used to replace $\boldsymbol{w}_k(n)$.

In some cases, it is advantageous to locally minimize the sum of the squared signals from only a few error sensors. This concept is formalized by employing independent weighting factors q_{km} to control the influence of the M error signals on each of the K adaptive filters [85]. The extreme case of this approach, $q_{km} \neq 0$ only if $k = m$ with $K = M$, has been examined [95] for a $1 \times 2 \times 2$ system. The stability of such a decentralized ANC system in a free field is achieved by positioning each error sensor closer to its associated secondary source than to the other secondary source.

2) Frequency-Domain Convergence Analysis: The convergence behavior of a multiple-channel ANC system can be analyzed in the frequency domain in terms of the convergence of the individual secondary signals, the cost function, and the control effort [92]. This frequency-domain analysis applies to narrow-band ANC systems that control one or more harmonics of periodic noise and provides insight into the physical process involved.

For controlling a narrow-band noise component of known frequency, the reference signal is a pure sinusoid, which in the frequency domain can be considered a constant of value $X = 1$. Thus from Fig. 20, by expressing the quantities in the frequency domain and omitting the frequency index for simplicity, we have $\boldsymbol{Y} = \boldsymbol{W}$. Therefore, the error signal is expressed as $\boldsymbol{E} = \boldsymbol{D} - \boldsymbol{S}\boldsymbol{W}$. The multiple-channel frequency-domain FXLMS algorithm is expressed as [92]

$$\boldsymbol{W}(n+1) = (\boldsymbol{I} - \mu \boldsymbol{S}^H \boldsymbol{S})\boldsymbol{W}(n) + \mu \boldsymbol{S}^H \boldsymbol{D} \tag{47}$$

where the superscript H (Hermitian) denotes conjugate transpose. Therefore, the matrix $\boldsymbol{S}^H\boldsymbol{S}$ plays the same role as the reference signal autocorrelation matrix in the single-channel case. The eigenvalues of $\boldsymbol{S}^H\boldsymbol{S}$ determine the convergence characteristics of the multiple-channel frequency-domain FXLMS algorithm. It is noteworthy that disparate eigenvalues arise here because of the spatial nature of the secondary-path matrix $\boldsymbol{S}$. Thus, the convergence of the general broad-band multiple-channel FXLMS algorithm is limited by both the spatial and temporal characteristics of the system.

As with the single-channel leaky FXLMS algorithm, the cost function can be modified to include the control effort, written as

$$\xi(n) = \boldsymbol{E}^H\boldsymbol{E} + \gamma \boldsymbol{W}^H\boldsymbol{W} \tag{48}$$

where γ is a real constant that determines the balance between reducing the total MSE $\boldsymbol{E}^H\boldsymbol{E}$ and moderating the control effort $\boldsymbol{W}^H\boldsymbol{W}$. The convergence of the multiple-channel frequency-domain leaky FXLMS algorithm is guaranteed if [92]

$$\mu < \frac{2}{\sigma_k^2 + \gamma}, \qquad k = 1, 2, \ldots, K \tag{49}$$

where σ_k^2 is the kth eigenvalue of $\boldsymbol{S}^H\boldsymbol{S}$. The effect of γ on the convergence of the ANC system is to speed up the very slow modes of convergence, which are associated with small values of σ_k^2, by adding a constant factor γ. (See [4] for further details.)

A suitably chosen value of γ will not only speed up convergence but can also prevent physically unreasonable values of control effort. The value of γ is selected to give the best tradeoff between controlling significantly excited modes and moderating the control effort expended on insignificant modes. Moderating the control effort also considerably reduces the risk of instability due to errors in the secondary-path models [34]. Furthermore, the constrained algorithm is equivalent to the leaky FXLMS algorithm, which has the additional benefit of reducing the effects of numerical errors and preventing algorithm stalling.

3) Feedback Reduction: As illustrated in Fig. 20, there is generally feedback from the K secondary sources to the J reference sensors. Therefore, the problems of reference signal contamination and possible system instability necessitate a modification of the multiple-channel FXLMS algorithm. Acoustic arrangements to reduce feedback are discussed in [4]. Another technique to reduce feedback from K secondary actuators to the reference sensor in the broad-band multiple-channel ANC system is to use feedback neutralization.

D. Multiple-Reference/Multiple-Output FXLMS Algorithm

The general multiple-reference/multiple-output ANC system using the FXLMS algorithm is shown in Fig. 20, where the ANC filter $\boldsymbol{W}$ has J reference input signals $x_j(n)$ that are elements of the signal vector $\boldsymbol{x}(n)$. Each controller in the matrix $\boldsymbol{W}$ is represented by $W_{kj}(z)$, where j is the reference input index and k is the secondary source index. The secondary signal output to the kth secondary source is

$$y_k(n) = \sum_{j=1}^{J} \boldsymbol{w}_{kj}^T(n)\boldsymbol{x}_j(n), \qquad k = 1, 2, \ldots, K \tag{50}$$

where $\boldsymbol{x}_j(n) \equiv [x_j(n)\ x_j(n-1)\cdots x_j(n-L+1)]^T, j = 1, 2, \cdots, J$ are the reference signal vectors. There are $M \times K$ different secondary paths $S_{mk}(z)$ between the secondary sources and error sensors, which are modeled by $\hat{S}_{mk}(z)$ to generate an array of filtered reference signals $x'_{jkm}(n)$ for the multiple-channel FXLMS algorithm

$$\boldsymbol{w}_{kj}(n+1) = \boldsymbol{w}_{kj}(n) + \mu \sum_{m=1}^{M} \boldsymbol{x}'_{jkm}(n)e_m(n) \tag{51}$$

for $k = 1, 2, \ldots, K$ and $j = 1, 2, \ldots, J$, where the vectors

$$\boldsymbol{x}'_{jkm}(n) \equiv \hat{s}_{mk}(n) * \boldsymbol{x}_j(n) \tag{52}$$

are the filtered reference signal vectors.

A practical application of multiple-reference/multiple-output active control for propeller blade-passage noise inside a 50-seat aircraft has been reported [33]. That system uses three reference signals (internally generated sinusoids) for the fundamental frequency and its first two harmonics, 16 secondary sources, and 32 error sensors, resulting in a 3 $\times$ 16 $\times$ 32 multiple-reference/multiple-output ANC system.

C. Multiple-Channel IIR Algorithm

The purpose of the broad-band feedforward multiple-reference/multiple-output adaptive IIR controller [41], [73], [96] is to provide multiple-channel ANC capability with longer impulse responses and feedback compensation using a low-order recursive section. As illustrated in Fig. 21, the controller contains two filter sections. The first section is a block of all-zero FIR filters from each reference sensor to each secondary source, while the second section implements a matrix-IIR structure of all-pole filters. The feedforward section of the controller is represented by the transfer function matrix $\boldsymbol{A}(z)$, which is composed of elements $A_{kj}(z)$ from input $x_j(n)$ to the kth summing node to produce $y_k(n)$, the kth component of the output vector $\boldsymbol{y}(n)$. Likewise, the transfer function matrix $\boldsymbol{B}(z)$ represents the recursive section of the controller with element $B_{ki}(z)$ from $y_i(n-1)$ to $y_k(n)$. Therefore, the secondary signal $y_k(n)$, which drives the kth secondary source, is expressed as

$$y_k(n) = \sum_{j=1}^{J} \boldsymbol{a}_{kj}^T(n)\boldsymbol{x}_j(n) + \sum_{i=1}^{K} \boldsymbol{b}_{ki}^T(n)\boldsymbol{y}_i(n-1) \quad \text{for } k = 1, 2, \ldots, K \tag{53}$$

where $\boldsymbol{a}_{kj}(n) \equiv [a_{kj,0}(n)\ a_{kj,1}(n)\cdots a_{kj,L-1}(n)]^T$ and $\boldsymbol{b}_{ki}(n) \equiv [b_{ki,0}(n)\ b_{ki,1}(n)\cdots b_{ki,I-1}(n)]^T$ are the feedforward and feedback filter coefficients, respectively, and $\boldsymbol{x}_j(n), \boldsymbol{y}_k(n)$ are, respectively, the reference input signal vectors and output signal vectors.

A multiple-reference/multiple-output filtered-U recursive LMS algorithm [41], [96] for the IIR filter structure minimizes the sum of the M MSE signals

$$\boldsymbol{a}_{kj}(n+1) = \boldsymbol{a}_{kj}(n) + \mu \sum_{m=1}^{M} \boldsymbol{x}'_{jkm}(n)e_m(n) \tag{54}$$

$$\boldsymbol{b}_{ki}(n+1) = \boldsymbol{b}_{ki}(n) + \mu \sum_{m=1}^{M} \boldsymbol{y}'_{ikm}(n)e_m(n) \tag{55}$$

where $\boldsymbol{x}'_{jkm}(n) \equiv \hat{s}_{mk}(n) * \boldsymbol{x}_j(n)$ and $\boldsymbol{y}'_{ikm}(n) \equiv \hat{s}_{mk}(n) * \boldsymbol{y}_i(n)$ are, respectively, the filtered reference and output signal vectors.

Multiple-channel adaptive IIR filtering has been successfully applied to the active control of random noise in a small reverberant room [41]. In that work, the performance of adaptive multiple-channel FIR and IIR filters was compared

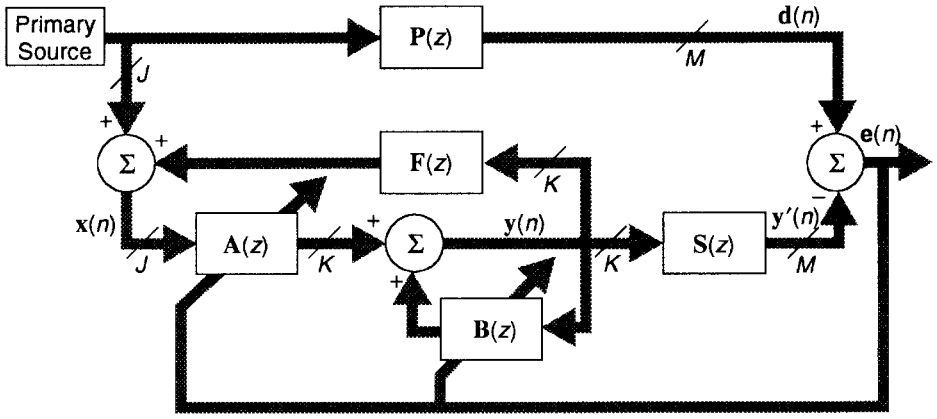

Fig. 21. Block diagram of multiple-channel ANC system using an IIR adaptive filter.

experimentally for an ANC system with four secondary sources and eight error sensors. The matrix-IIR structure results in a more stable configuration in the presence of feedback, especially if a small leakage factor is included. The experimental results also show that far better performance is achieved by using IIR filters rather than FIR filters when the primary noise source has a lightly damped dynamic behavior.

D. Multiple-Channel Adaptive Feedback ANC Systems

The single-channel feedback ANC system shown in Fig. 15 is easily extended to a $K \times 1$ system that has K secondary sources and one error sensor. The reference signal $x(n)$ of the feedback ANC system is synthesized as an estimate of the primary noise

$$x(n) \equiv \hat{d}(n) = e(n) + \sum_{k=1}^{K} \hat{s}_k(n) * y_k(n) \tag{56}$$

where $\hat{s}_k(n)$ is the impulse responses of filter $\hat{S}_k(z)$, which models the secondary path $S_k(z)$ from the kth secondary source to the error sensor and $y_k(n)$ are the secondary signals obtained from the adaptive filters $W_k(z)$.

The FXLMS algorithm is used to minimize the error signal $e(n)$ by adjusting the weight vector for each adaptive filter $W_k(z)$ according to

$$\boldsymbol{w}_k(n+1) = \boldsymbol{w}_k(n) + \mu \boldsymbol{x}'_k(n) e(n), \qquad k = 1, 2, \ldots, K \tag{57}$$

where

$$\boldsymbol{x}'_k(n) \equiv \hat{s}_k(n) * \boldsymbol{x}(n) \tag{58}$$

is the reference signal vector filtered by the secondary-path estimate $\hat{S}_k(z)$.

A more general $K \times M$ adaptive feedback ANC system is illustrated in Fig. 22. In this system, there are $M \times K$ secondary paths $S_{mk}(z)$ from the kth secondary source to the mth error sensor, which are estimated by the corresponding filters $\hat{S}_{mk}(z)$. The reference signal synthesizer uses the K secondary signals $y_k(n)$, M error signals $e_m(n)$, and $M \times K$ secondary-path estimates $\hat{S}_{mk}(z)$ to generate

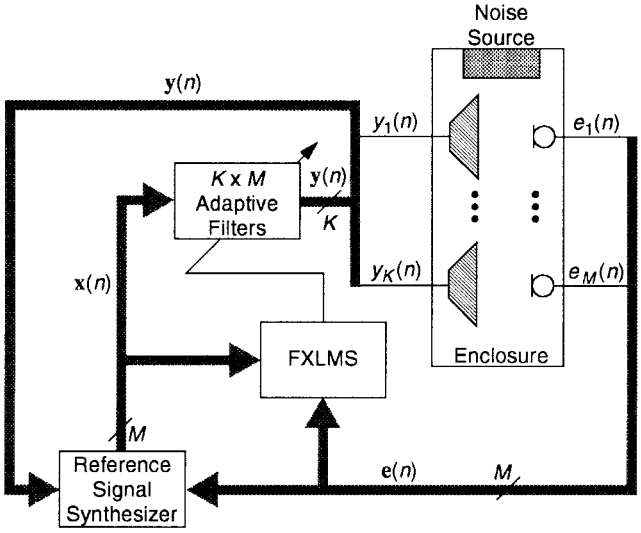

Fig. 22. Block diagram of $K \times M$ feedback ANC system.

M reference signals $x_m(n)$ for the corresponding $K \times M$ adaptive filters, $W_{km}(z)$. The synthesized reference signals are expressed as

$$x_m(n) = e_m(n) + \sum_{k=1}^{K} \hat{s}_{mk}(n) * y_k(n), \qquad m = 1, 2, \ldots, M \tag{59}$$

where $\hat{s}_{mk}(n)$ is the impulse response of the secondary-path estimate $\hat{S}_{mk}(z)$. The coefficients are updated by the multiple-channel $(J \times K \times M)$ FXLMS algorithm discussed in Section V-C for the special case $J = M$. The multiple-channel adaptive feedback ANC system was applied to reduce noise in the operator cabin of a tractor [97] and in a large dimension duct [98].

VI. Online Secondary-Path Modeling

As discussed in previous sections, the secondary path is estimated offline prior to the operation of the ANC system. For some applications the secondary path may be time varying, and it is desirable to estimate the secondary path online when the ANC is in operation.

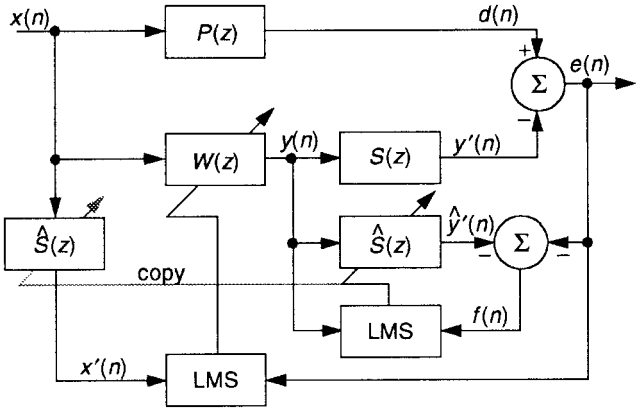

Fig. 23. Block diagram of online secondary-path modeling technique proposed in [9].

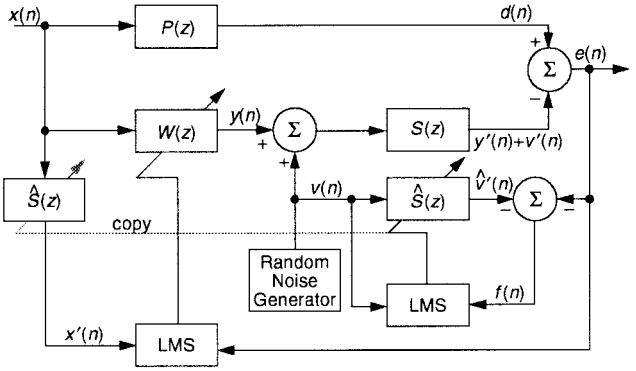

Fig. 24. Block diagram of ANC system with online secondary-path modeling using additive random noise.

A. Fundamental Problem

An ANC system using the FXLMS algorithm with adaptive online secondary-path modeling [9] is illustrated in Fig. 23. The adaptive filter $W(z)$ generates a secondary noise $y(n)$ that passes through the secondary path $S(z)$, which is modeled by the adaptive filter $\hat{S}(z)$ connected in parallel with the secondary path. In this scheme, the secondary signal $y(n)$ also serves as an excitation signal for secondary-path modeling. The coefficients of the adaptive filter $\hat{S}(z)$ are adjusted online to model continuously the secondary path $S(z)$ during the operation of ANC filter $W(z)$. Assuming that $\hat{S}(z)$ is of sufficient order, that $x(n)$ is a persistent excitation signal, and that $P(z)$ and $S(z)$ are time-invariant systems, the steady-state solution of $\hat{S}(z)$ is [4]

$$\hat{S}^{o}(z) = S(z) - \frac{P(z)}{W(z)}. \tag{60}$$

This equation shows that the estimate $\hat{S}(z)$ obtained by the online modeling algorithm of Fig. 23 is biased by $P(z)/W(z)$. The adaptive filter $\hat{S}(z)$ can correctly identify $S(z)$ only if $P(z) = 0$ [or equivalently, $d(n) = 0$]. Equation (60) also shows that $\hat{S}^{o}(z)$ is affected by the adaptive filter $W(z)$. From (3), the optimum solution of $W(z)$ is $W^{o}(z) = P(z)/S(z)$, that is, an inverse model of the secondary-path transfer function $S(z)$. Therefore, the interaction between adaptive filters $W(z)$ and $\hat{S}(z)$ is very complicated. For example, by substituting $W^{o}(z)$ into (60), we have $\hat{S}^{o}(z) = 0$, which is an undesired solution and should be avoided.

There are two important requirements of secondary-path modeling. The first is that an accurate estimate of $S(z)$ should be produced, regardless of the controller transfer function $W(z)$. This independence property will ensure that the overall ANC system is robust. The second requirement is that the adaptive filter $\hat{S}(z)$ should not intrude on the operation of the ANC system. These two properties appear to be mutually exclusive because in order to obtain an accurate and independent estimation of $S(z)$, it would be preferable for the modeling filter $\hat{S}(z)$ to manipulate the excitation (secondary) signal $y(n)$ directly. However, for the $\hat{S}(z)$ to be unobtrusive, it should observe only the signals already in the system. Consequently, in a practical ANC system, a tradeoff between independence and intrusion has to be resolved.

B. Additive Random Noise Technique

1) Basic Technique and Convergence Analysis: An online secondary path modeling technique using additive random noise [99] is illustrated in Fig. 24. A zero-mean white noise $v(n)$ is internally generated and is added to the secondary signal $y(n)$ to drive the secondary source. The adaptive filter $\hat{S}(z)$ is connected in parallel with the secondary path $S(z)$; however, the input signal used for $\hat{S}(z)$ is the random noise $v(n)$ only.

It is useful to define the component of the error due to the original noise as

$$\begin{aligned} u(n) &\equiv d(n) - s(n) * y(n) \\ &= [p(n) - s(n) * w(n)] * x(n) \end{aligned} \tag{61}$$

where $p(n), s(n)$, and $w(n)$ are the impulse responses of $P(z), S(z)$, and $W(z)$ at time n. Since $x(n)$ is uncorrelated with $v(n), u(n)$ is also uncorrelated with $v(n)$. Therefore, the LMS solution is unaffected by the presence of the interference $u(n)$. However, $u(n)$ will have an effect on the convergence of the adaptive algorithm.

As illustrated in Fig. 24, the coefficients of the adaptive filter $\hat{S}(z)$ are updated by the LMS algorithm, which is expressed as [4]

$$\begin{aligned} \hat{\boldsymbol{s}}(n+1) &= \hat{\boldsymbol{s}}(n) + \mu \boldsymbol{v}(n) f(n) \\ &= \hat{\boldsymbol{s}}(n) + \mu \boldsymbol{v}(n)[v'(n) - \hat{v}'(n)] - \mu \boldsymbol{v}(n) u(n) \end{aligned} \tag{62}$$

where $\hat{\boldsymbol{s}}(n)$ is the coefficient vector of $\hat{S}(z)$ and $\boldsymbol{v}(n)$ is the reference signal vector. The expected value of $\hat{\boldsymbol{s}}(n)$ in (62) converges to its optimal solution $\boldsymbol{s}(n)$, provided $v(n)$ and $u(n)$ are uncorrelated. However, this does not mean that instantaneous values of $\hat{\boldsymbol{s}}(n)$ will be equal to $\boldsymbol{s}(n)$. It is obvious that the undesired term $\mu \boldsymbol{v}(n) u(n)$ in (62) is a disturbance that is frustrating convergence of the LMS algorithm and will therefore degrade the performance of the adaptive filter $\hat{S}(z)$.

For online modeling, $u(n)$ acts like an uncorrelated plant noise of power σ_u^2. After convergence, this residual noise due to $u(n)$ will perturb the adaptive weights of $\hat{S}(z)$, resulting in a misalignment, or mean-square modeling error, that is given by [9]

$$\sigma_{\hat{s}}^2 \equiv \lim_{n\to\infty} E\sum_{m=0}^{M-1}[\hat{s}_m(n)-s_m(n)]^2 \approx \frac{\mu}{2}M\sigma_u^2 \qquad (63)$$

where $\hat{s}_m(n)$ and $s_m(n), m = 0,1,\ldots,M-1$ are the impulse responses of the filters $\hat{S}(z)$ and $S(z)$, respectively.

For offline modeling, $u(n) = 0$ and (62) will converge for sufficiently small step size μ. The step size bound for fastest convergence is $\mu_{\text{off}} = 2/(3M\sigma_v^2)$, where M is the order of the adaptive filter $\hat{S}(z)$ and σ_v^2 is the variance of the white noise $v(n)$ [4]. As an example, suppose that an online normalized modeling error $\sigma_{\hat{s}} = 0.1$ (-20 dB) was specified. Then the step size is limited to the value $\mu_{\text{on}} = 2/(300M\sigma_v^2)$ [4]. Therefore, it would take 100 times as long for $\hat{S}(z)$ to converge online as it would to converge offline. In most ANC applications, the interference $u(n)$ is much larger than the excitation signal $v(n)$ and the convergence rate of filter $\hat{S}(z)$ is therefore very slow, or it may fail to converge because of finite-wordlength effects.

2) Methods for Improvement: To improve the convergence of $\hat{S}(z)$ in the presence of the interference $u(n)$, the adaptive noise cancellation technique [56] can be used to cancel the component of $e(n)$ that is correlated with the primary source $x(n)$ [100], [101]. An additional adaptive filter with $x(n)$ as the reference signal is used to cancel the undesired component $u(n)$ in error signal $e(n)$ picked up by the error sensor. The convergence rate of the modeling filter $\hat{S}(z)$ has been shown to improve by a factor of $\sim$30 using this technique. A limitation of this technique is its inability to cancel any interference that is uncorrelated with $x(n)$. This problem can be solved by using an adaptive prediction error filter to reduce the interference $u(n)$ in error signal $e(n)$ [102]. The optimum delay for the adaptive predictor is equal to the length of the impulse response of the secondary path being modeled.

C. Overall Modeling Algorithm

An overall online secondary-path modeling algorithm [49], [103]–[105] tries to eliminate the biasing term $P(z)/W(z)$ in (60) by introducing another adaptive filter $\hat{P}(z)$ to model $P(z)$. The output of $\hat{P}(z)$ is then used to cancel the disturbance $d(n)$ that is the output signal of $P(z)$. Altogether, the complete ANC system uses three adaptive filters—$W(z), \hat{S}(z)$, and $\hat{P}(z)$—to perform noise control and secondary-path modeling simultaneously. This algorithm has the capability to model the secondary path without using an additional excitation signal. However, the convergence of this algorithm depends on the secondary signal, and there is no unique solution for both adaptive filters $\hat{S}(z)$ and $\hat{P}(z)$. An offline initialization procedure [106] uses delay z^{-L} to decorrelate the primary and secondary signals so that $\hat{S}(z)$ and $\hat{P}(z)$ will converge to $S(z)$ and $P(z)$, respectively.

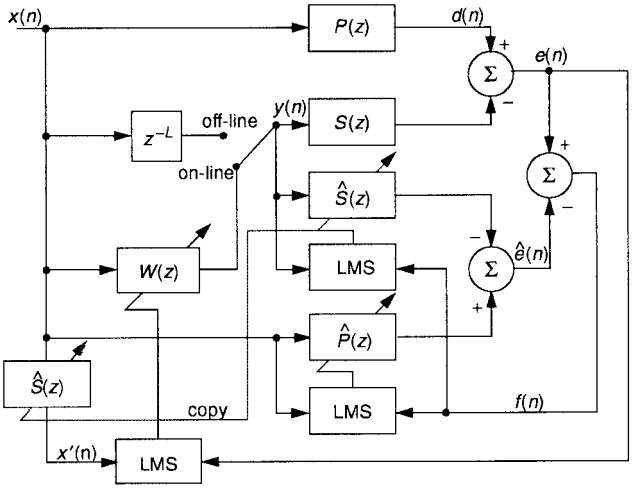

Fig. 25. ANC system using overall modeling technique.

The complete ANC system using this secondary-path modeling algorithm is illustrated in Fig. 25. The secondary signal is switched between the outputs of $W(z)$ and z^{-L}. The delay z^{-L} is used during the initialization stage or if significant changes in $P(z)$ and/or $S(z)$ are detected, at which times only $\hat{S}(z)$ and $\hat{P}(z)$ are updated. Otherwise the system updates $W(z), \hat{S}(z)$, and $\hat{P}(z)$ to perform ANC and online secondary-path modeling simultaneously using the secondary signal from $W(z)$ as the excitation signal. The implementation of z^{-L} costs only one delay unit because $L-1$ delay units are already included in $W(z)$.

After $\hat{P}(z)$ and $\hat{S}(z)$ have converged, we have [4]

$$P(z) - S(z)z^{-L} = \hat{P}(z) - \hat{S}(z)z^{-L} \qquad (64)$$

assuming that $x(n)$ provides sufficient excitation at all frequencies. Therefore, the corresponding $\hat{P}(z) = P(z)$ and $\hat{S}(z) = S(z)$. The accuracy of this overall modeling algorithm depends on the order of $\hat{S}(z)$ and $\hat{P}(z)$ and the length of the impulse response of $P(z)$ and $S(z)$. Since the impulse responses of stable physical systems exhibit exponential decay, the modeling errors may be neglected if the order of $\hat{S}(z)$ and $\hat{P}(z)$ are large. Adaptive filters $\hat{S}(z)$ and $\hat{P}(z)$ are able to track $S(z)$ and $P(z)$, respectively, if only one is changing at a time. Extensive simulations using measured transfer functions from a real experimental setup show that $\hat{P}(z)$ and $\hat{S}(z)$ are able to track "slow" changes in both $P(z)$ and $S(z)$ online when $W(z)$ is used [107].

D. Multiple-Channel Modeling Algorithms

1) Interchannel Coupling Effect: Online modeling of $K \times M$ secondary paths is more difficult than for a single-channel case, since the error signal $e_m(n)$ from the mth error sensor is a mixture of signals coming from the primary path $P_m(z)$ and secondary paths $S_{mk}(z)$ for $k = 1,2,\ldots,K$. To explain the effect of interchannel coupling, consider the $1 \times 2 \times 2$ ANC system illustrated in Fig. 26. The secondary signals $y_1(n)$ and $y_2(n)$ are generated by adaptive filters and are combined with additive random noise $v(n)$ to drive the secondary sources. The error

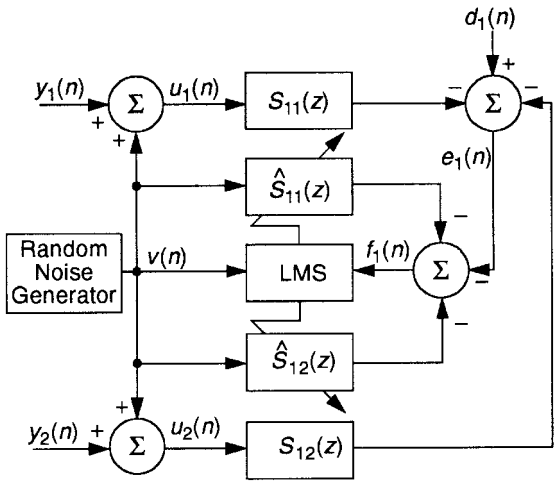

Fig. 26. Secondary-path modeling for a $1 \times 2 \times 2$ ANC system using one random noise generator.

signal $e_1(n)$ is measured by the first error sensor, which is the residual error of the primary noise $d_1(n)$ canceled by the noises from both secondary sources. Adaptive filters $\hat{S}_{11}(z)$ and $\hat{S}_{12}(z)$ are used to model the secondary paths $S_{11}(z)$ and $S_{12}(z)$, respectively.

Assuming that the excitation signal $v(n)$ is zero mean and is uncorrelated with $y_1(n), y_2(n)$, and $d_1(n)$, the adaptive filter $\hat{S}_{11}(z)$ will converge to [4]

$$\hat{S}_{11}^{o}(z) = S_{11}(z) + \left[S_{12}(z) - \hat{S}_{12}(z)\right]. \qquad (65)$$

This equation shows that when random noise components are picked up by the first error sensor through multiple secondary paths [$S_{11}(z)$ and $S_{12}(z)$ in this case], the estimate $\hat{S}_{11}(z)$ is biased by the cross-coupled secondary paths $S_{12}(z)$ and $\hat{S}_{12}(z)$. Furthermore, since $\hat{S}_{12}(z)$ is adapted at the same time as $\hat{S}_{11}(z)$, there is no unique solution for either filter. Note that this cross-coupling effect occurs for both online and offline modeling.

2) Multiple-Channel Online Modeling Algorithms: If only one random noise generator is used, only M secondary paths from one of the secondary sources to the M error sensors can be estimated at a time, since each of the K secondary sources couples to each error sensor. This process is repeated K times by injecting a random noise sequentially into one secondary source at a time, thereby obtaining estimates of the $K \times M$ secondary path transfer functions. A shortcoming of this solution is the total time required to model all the secondary paths (both offline and online), which may be too long for some ANC applications.

An alternative solution is to use, for example, two random noise generators [4] for a $1 \times 2 \times 2$ system. The random noises $v_1(n)$ and $v_2(n)$ are mutually uncorrelated and also uncorrelated with other signals. This technique can be generalized to solve the interchannel coupling problem of a $J \times K \times M$ ANC system using K independent random noise generators. However, the cost may be too high for some ANC applications. An interchannel decoupling algorithm [108] uses a single noise generator with interchannel delay to decorrelate the excitation signals. This technique allows simultaneous off-line or online modeling of $K \times M$ secondary paths using a single random noise generator.

The overall modeling algorithm discussed in Section VI-C can also be extended to multiple-channel ANC systems with M error signals and $K+1$ adaptive filters for each error signal, where K is the number of secondary sources. For each error signal, K adaptive filters $\hat{S}_{mk}(z), k = 1, 2, \ldots, K$ are used to model the corresponding secondary paths $S_{mk}(z)$ and combined with an adaptive filter $\hat{P}_m(z)$ to cancel the highly correlated disturbance $d_m(n)$ from the primary noise source. This multiple-channel ANC algorithm was applied to control structural vibration [109].

3) Audio Interference Cancellation: An integrated ANC-audio system enhances a desired audio signal by utilizing ANC to reduce unwanted acoustic noise. This integrated system uses shared analog components such as mixers, amplifiers, and loudspeakers so that multiple-channel ANC may be applied in a variety of applications, such as automobiles, without the expense of system redundancies. In this integrated system, the audio signal picked up by the error sensors in an enclosure becomes an interference to the ANC system. The audio interference to the ANC filter can be reduced using an adaptive noise canceler with the desired audio signal as the reference signal [110]. Assuming that the audio signal is of persistent excitation and uncorrelated with the primary noise, the adaptive filter used for the audio interference cancellation will converge to the secondary path, and thus also performs online secondary-path modeling. In addition, music would be more enjoyable than random noise, both in the initial training stage and for online operation. This integrated system is expanded to incorporate hands-free cellular phone operation [111].

Interference cancellation and online modeling are inherently more difficult for the multiple-channel case. First, the left and right audio signals may be partially correlated and that would cause problems in uniquely identifying the cross-coupled secondary paths. Furthermore, the interchannel decoupling delay technique cannot be used here because that would destroy the stereo effect of the desired signals. Consequently, offline techniques or some combination of online and offline techniques would have to be employed for multiple-channel systems.

VII. Other ANC Structures and Algorithms

The adaptive transversal filter using the FXLMS algorithm is the most widely used technique for ANC systems, owing to its simplicity and robustness. However, the LMS algorithm has the disadvantage of relatively slow and signal-dependent convergence. This may be only a minor problem for ANC systems with stationary noise sources such as transformers, electric power generators, diesel-powered boats, locomotives, and compressors. For nonstationary noise sources such as automobiles, slow convergence is a critical problem when attempting to cancel transient noise, which occurs at vehicle startups, stops, or gearshifts, or with sudden changes of engine speeds or road noise from tires.

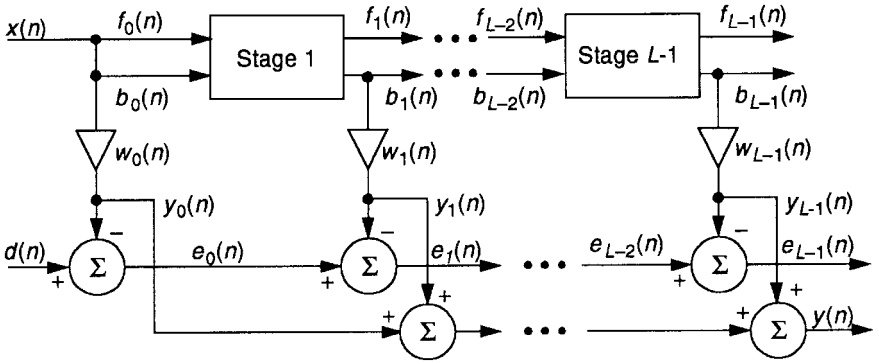

Fig. 27. Overall structure of lattice predictor and multiple regression filter.

An adaptive system involves two basic parts: a filtering operation that produces an output signal and an adaptation algorithm that adjusts the coefficients of the filter. If a transversal filter is used, the convergence rate can be improved by using more advanced algorithms such as adjustable-step-size LMS algorithms and recursive-least-squares (RLS) algorithm. The other approach is to condition the reference signal by employing different filter structures such as the lattice filter, subband filter, or orthogonal transform.

The simplest approach for improving the convergence of the LMS algorithm is to use adaptive step sizes [112]–[115]. The selection of step size can be based on the magnitude of the error signal, polarity of successive samples of the error signal, measurement of the correlation of the error signal with the reference signal, and other features. The performance of these techniques is highly dependent on the selection of certain parameters in the algorithms, and the optimal choice is highly signal dependent. A variable-step-size LMS algorithm was used to improve convergence for an air-conditioning duct ANC application [116], [117].

A. Lattice ANC

1) Lattice Structures and Algorithms: The adaptive lattice predictor is a modular structure that consists of a number of cascaded stages with two input and two output channels. The lattice structure enjoys the advantages of a simple test for filter stability, good performance in finite-wordlength hardware implementations, and greatly reduced sensitivity to the eigenvalue spread of the reference signal [15]. The recursive equations that describe the lattice structure are expressed as [4]

$$f_l(n) = f_{l-1}(n) - k_l(n) b_{l-1}(n-1) \qquad l = 1, 2, \ldots, L-1 \tag{66}$$

$$b_l(n) = b_{l-1}(n-1) - k_l(n) f_{l-1}(n) \qquad l = 1, 2, \ldots, L-1 \tag{67}$$

where $f_l(n)$ is the forward prediction error, $b_l(n)$ is the backward prediction error, $k_l(n)$ is the reflection coefficient, n is the time index, l is the stage (order) index, and $L-1$ is the total number of cascaded stages. The reference signal $x(n)$ is used as the input signal for stage one, as shown in Fig. 27 and expressed by $f_0(n) = b_0(n) = x(n)$.

The reflection coefficients $k_l(n)$ of adaptive filter are updated by the gradient lattice algorithm to minimize the mean square of the sum of forward and backward prediction errors at each stage [118], [119]

$$k_l(n+1) = k_l(n) + \mu_l [f_l(n) b_{l-1}(n-1) + b_l(n) f_{l-1}(n)] \qquad l = 1, 2, \cdots, L-1 \tag{68}$$

where μ_l is the step size of the lth stage. The steady-state reflection coefficients of the lattice predictor have a magnitude less than one [15]. This property is very important and convenient for a fixed-point hardware implementation. Another important property of the lattice structure is that the backward prediction errors $b_l(n)$ are mutually uncorrelated [15]. Thus, the lattice predictor transforms the correlated reference signals $\{x(n)\ x(n-1) \cdots x(n-L+1)\}$ into a corresponding sequence of uncorrelated backward prediction errors $\{b_0(n)\ b_1(n) \cdots b_{L-1}(n)\}$. The multiple regression filter with coefficients $\{w_0(n)\ w_1(n) \cdots w_{L-1}(n)\}$ then operates on the backward prediction errors to produce a filter output $y(n)$.

As shown in Fig. 27, the regression filter is formed as

$$e_l(n) = e_{l-1}(n) - b_l(n) w_l(n), \qquad l = 1, 2, \cdots, L-1 \tag{69}$$

where $d(n)$ is the primary signal and $e_0(n) = d(n) - b_0(n) w_0(n)$. The output signal is formed as

$$y(n) = \sum_{l=0}^{L-1} w_l(n) b_l(n). \tag{70}$$

The coefficients of the regression filter are updated by the LMS algorithm, expressed as

$$w_l(n+1) = w_l(n) + \mu b_l(n) e_l(n), \qquad l = 0, 1, \ldots, L-1. \tag{71}$$

2) Lattice ANC Systems: A lattice ANC system using the FXLMS algorithm is illustrated in Fig. 28. The placement of the secondary path $S(z)$ following the adaptive regression filter results in the FXLMS algorithm, expressed as [4]

$$\boldsymbol{w}(n+1) = \boldsymbol{w}(n) + \mu \boldsymbol{b}'(n) e(n) \tag{72}$$

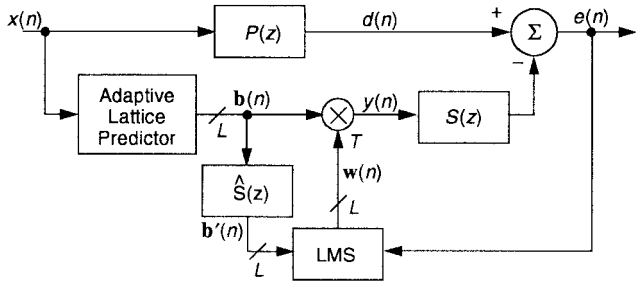

Fig. 28. ANC system using a lattice filter and the FXLMS algorithm.

where $\boldsymbol{b}'(n) \equiv [b'_0(n)\ b'_1(n) \cdots b'_{L-1}(n)]^T$ is the filtered backward prediction error vector with elements

$$b'_l(n) = \hat{s}(n) * b_l(n) = \sum_{m=0}^{M-1} \hat{s}_m b_l(n-m) \qquad l = 0, 1, \ldots, L-1. \tag{73}$$

The lattice ANC system converges significantly faster than the traditional transversal filter ANC when the primary noise consists of sinusoidal components with widely differing power [120].

The computation of $b'_l(n)$ for $l = 0, 1, \ldots, L-1$ expressed in (73) requires intensive computation and storage since each $b_l(n), l = 0, 1, \ldots, L-1$ is filtered by the secondary-path estimate $\hat{S}(z)$. In order to reduce the computation and memory requirements, the algorithm shown in Fig. 28 is modified in [121], where the reference signal $x(n)$ is first filtered by $\hat{S}(z)$, yielding $x'(n)$. This filtered signal is then passed through a second lattice filter with input $f_0(n) = b_0(n) = x'(n)$ and the reflection coefficients $k_l(n)$ are copied from the adaptive lattice predictor shown in Fig. 28. This slaved lattice filter then generates L signals $b'_l(n)$, which are used for the FXLMS algorithm in (72) to update the regression weights.

B. Frequency-Domain ANC

The frequency-domain adaptive filter [122], [123] transforms the primary and reference signals into the frequency domain using the fast Fourier transform (FFT) and processes these signals by an adaptive filter. This frequency-domain technique saves computations by replacing the time-domain linear convolution by multiplication in the frequency domain. In this section, we use the FFT to illustrate the basic idea of frequency-domain adaptive filters. However, in most practical ANC applications, the physical signals are real-valued. Therefore, the real-valued discrete cosine or discrete Hartley transforms [124], [125] may be more convenient from an implementational point of view.

A frequency-domain FXLMS algorithm for ANC is illustrated in Fig. 29. The reference signal, $x(n)$, is stored in an L-point data buffer and then transformed to the frequency-domain signals $X_l(n)$ using the FFT. These frequency-domain reference signals are filtered by the corresponding adaptive weights $W_l(n)$ to produce the frequency-domain output signals $Y_l(n)$. These output signals are then processed by an inverse FFT to obtain the time-domain output

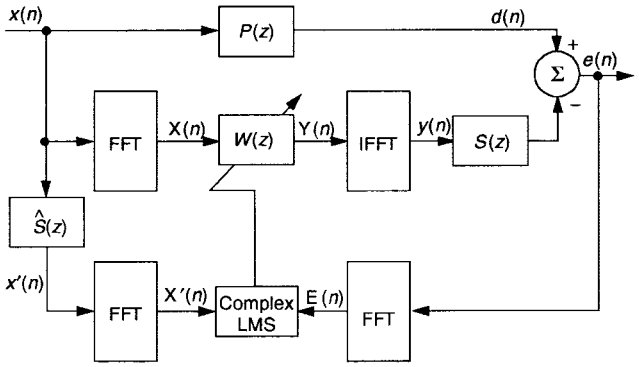

Fig. 29. Frequency-domain FXLMS algorithm for ANC.

signals $y(n)$. The output signals in the data buffer are sequentially output to the secondary source, one at each sampling period. In Fig. 29, $x(n)$ is also filtered by $\hat{S}(z)$ to yield $x'(n)$, which is stored in an L-point data buffer. This filtered reference signal vector is then transformed into the frequency domain $X'_l(n)$ using the FFT. The residual error $e(n)$ measured by the error sensor is also stored in an L-point data buffer and transformed to obtain $E_l(n)$.

Since the reference signal $x(n)$ has been split into L frequency bins, considerable improvement in convergence is achieved by using an individual step size $\mu_l(n)$ for each frequency bin that is inversely proportional to the signal power at that bin. This results in the normalized frequency-domain FXLMS algorithm expressed as

$$W_l(n+L) = W_l(n) + \mu_l(n) X'^{*}_l(n) E_l(n) \qquad l = 0, 1, \ldots, L-1 \tag{74}$$

where $X'^{*}_l(n)$ is the complex conjugate of $X'_l(n)$

$$\mu_l(n) = \frac{\mu}{P_l(n)}, \qquad l = 0, 1, \ldots, L-1 \tag{75}$$

is the normalized step size at frequency bin l, and

$$P_l(n) = (1-\alpha) P_l(n-L) + \alpha |X_l(n)|^2 \tag{76}$$

is a lowpass-filtered estimate of the power of $X_l(n)$. Note that this power estimate is also updated every block of L samples.

Instead of filtering the signal sample by sample, the frequency-domain FXLMS algorithm processes the signal block by block. Thus, there are L samples of delay between the input of the reference signal and the output of the secondary signal. This problem would be a shortcoming for the frequency-domain ANC system in controlling broad-band random noise because of the causality constraint. A frequency-domain implementation of the FXLMS algorithm has been developed [126], [127] and was extended to the multiple-channel case in [128].

C. Subband ANC

Broad-band ANC can often involve adaptive filter lengths with hundreds of taps [3]. A related problem occurs in the field of acoustic echo cancellation, where room acoustics involve long impulse responses [129]. One technique that

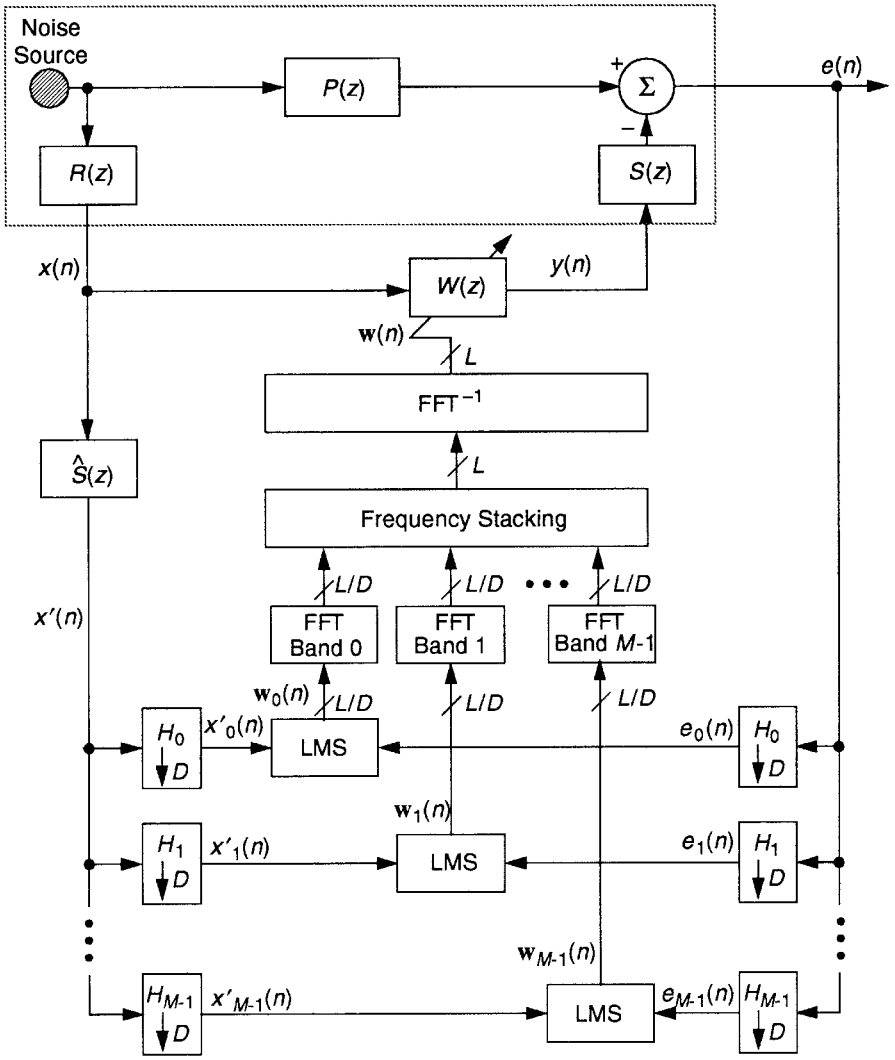

Fig. 30. Delayless subband ANC system.

has been recently advanced for that application involves the use of subbands [129], [130]. Processing the signals in subbands has a twofold advantage: 1) the computational burden is reduced by approximately the number of subbands, since both the number of taps and weight update rate can be decimated in each subband and 2) faster convergence is possible because the spectral dynamic range is greatly reduced in each subband. Unfortunately, the bandpass filters used in subband processing will introduce a substantial delay in the secondary path.

A modification of the subband technique eliminates delay in the secondary path [131], [132]. The basic idea is that the adaptive weights are computed in subbands but are then collectively transformed into an equivalent set of wideband filter coefficients. Fig. 30 shows the basic configuration of the delayless subband ANC technique. The disturbance and reference are assumed to be derived from a common noise source through the linear transfer functions $P(z)$ and $R(z)$, respectively. The wideband weight $W(z)$ is developed as a transformation of filtered-X derived subband weights, thereby eliminating any delay associated with the cancellation signal.

The filtered reference signal $x'(n)$ and error signal $e(n)$ are decomposed into sets of subband signals using the bandpass filters $H_0, H_1, \ldots, H_{M-1}$. In each subband, the signals are decimated by a factor D (possibly after appropriate band shifting) and the subband adaptive weights are computed by the complex LMS algorithm. The adaptive weights in each subband are then transformed into the frequency domain, appropriately stacked, and inverse-transformed to obtain the wideband filter coefficients. One way to implement the delayless subband adaptive filter is to employ the polyphase FFT technique [123]. A general formulation of the computational requirements in terms of the adaptive filter length, number of subbands, and polyphase filter length can be found elsewhere [132].

D. RLS Algorithm for ANC

The RLS algorithm can be used with an adaptive transversal filter to provide faster convergence and smaller steady-state error than the LMS algorithm. The "fast transversal filter" [133] is an efficient version of the RLS algorithm, which reduces the required operations to approximately $7L$. Haykin has given a detailed treatment of

RLS algorithms and the fast transversal filter [15]. We now show how the RLS algorithm can be modified for ANC applications, which incorporates a secondary path following the transversal filter. This method can also be applied to modify the fast transversal filter for ANC applications.

The least-squares method assumes a cost function at time n that consists of the sum of weighted error squares expressed by $\xi(n) = \Sigma_{i=1}^{n} \lambda^{n-i} e^2(i)$, where $0 \leq \lambda < 1$ is a forgetting (weighting) factor, which weights recent data more heavily in order to accommodate nonstationary signals. The fast RLS algorithm is developed by applying a time-recursive approach to computing $\boldsymbol{Q}(n) = \boldsymbol{R}^{-1}(n)$ from the previous $\boldsymbol{R}^{-1}(n-1)$, instead of estimating $\boldsymbol{R}(n)$ and then inverting it to obtain $\boldsymbol{R}^{-1}(n)$, where the sample autocorrelation matrix is defined as $\boldsymbol{R}(n) = \Sigma_{i=1}^{n} \lambda^{n-1} \boldsymbol{x}(i) \boldsymbol{x}^T(i)$.

The filtered-X RLS (FXRLS) algorithm for ANC is summarized as [4]

$$\boldsymbol{w}(n+1) = \boldsymbol{w}(n) + \boldsymbol{k}'(n) e(n) \tag{77}$$

$$\boldsymbol{k}'(n) = \frac{\boldsymbol{z}'(n)}{\boldsymbol{x}'^T(n) \boldsymbol{z}'(n) + 1} \tag{78}$$

$$\boldsymbol{z}'(n) = \lambda^{-1} \boldsymbol{Q}'(n-1) \boldsymbol{x}'(n) \tag{79}$$

$$\boldsymbol{Q}'(n) = \lambda^{-1} \boldsymbol{Q}'(n-1) - \boldsymbol{k}'(n) \boldsymbol{z}'^T(n) \tag{80}$$

where $\boldsymbol{x}'(n) \equiv [x'(n)\ x'(n-1) \cdots x'(n-L+1)]^T$ is the filtered reference signal vector with elements $x'(n) \equiv \hat{s}(n) * x(n)$.

E. Modal ANC

Modal decomposition for active control problems [134] offers a number of practical advantages. First, if an active control problem is known to involve only a few significant modes, then independent modal control can minimize the number of secondary sources, sensors, and corresponding dimensionality of the controller, as well as minimize the control energy [135]. Second, it is also known that modal control offers advantages of robustness to system parameter uncertainty and errors arising from spatial discretization [136], [137]. Finally, if the LMS algorithm is employed, the convergence time problem is minimized by uncoupling the modal responses.

The major topics to be addressed in a narrow-band modal ANC system deal with modal filters, secondary prefilters, spatial sampling effects, and design methodology [138]. Modal filters are intended to obtain from sensor measurements a best estimate of the coefficients, or participation factors, of certain desired modes, while rejecting as nearly as possible interference from other modes. Least-square prefilters are used with a set of mode-coupled secondary sources to synthesize desired modal amplitudes. Spatial sampling effects refer to the performance degradation that results from using a finite number of sensors. Finally, the design methodology develops a systematic approach to realize the most efficient modal ANC system.

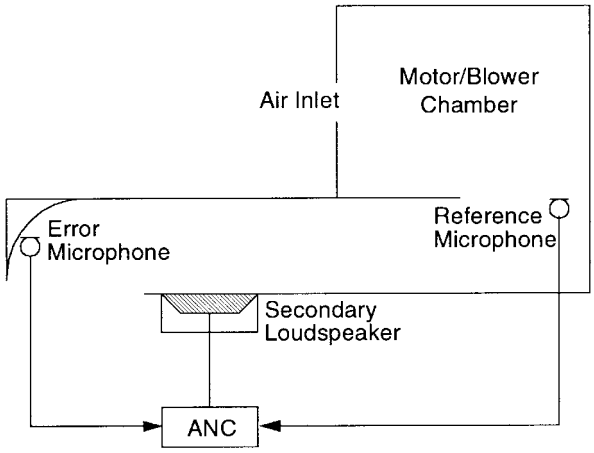

Fig. 31. ANC system for motor/blower (adapted from [139]).

VIII. ANC Applications

Many commercial applications of ANC have been developed in reducing noise for both industrial and domestic applications. General applications of air-acoustic, hydroacoustic, and vibrational ANC systems were introduced in Section I-B. In this section, we focus on some particular applications.

A. Single-Channel Broad-Band Feedforward Systems

Most successful ANC applications at present are single-channel systems for controlling low-frequency acoustic noise in narrow ducts or small cavities. Several design issues, such as coherence and causality, are critical for the success of broad-band ANC systems in practical applications.

1) Duct-Acoustic Noise: Single-channel broad-band feedforward ANC systems are ideal for one-dimensional ducts or pipework used in heating, ventilation, and air conditioning (HVAC). Because ANC system components are located outside the duct without inhibiting the airflow, there is no adverse effect on the fan speed or capacity. The ANC system can be installed quickly, even in tight places, and does not require major modifications to the existing ductwork. Typically, these ANC systems use an adaptive IIR filter with the filtered-U recursive LMS algorithm, as discussed in Section II-D2. An example of a single-channel broad-band ANC system is shown in Fig. 31, where the reference sensor is located in the duct at a position close to the motor/blower, while the error sensor is located near the discharge of the duct [139]. A secondary loudspeaker is mounted on the duct wall near the error sensor. This ANC system is based on the single-channel FXLMS algorithm discussed in Section II-C1. Other applications are discussed in [4].

2) Room-Acoustic Noise: Consider the acoustic ANC problem diagrammed in Fig. 32. A primary noise source on the right generates acoustic noise in an enclosed room. It is desired to create a "quiet zone" on the left side by sending a control signal to a secondary loudspeaker that produces a canceling acoustic signal. A microphone on the left

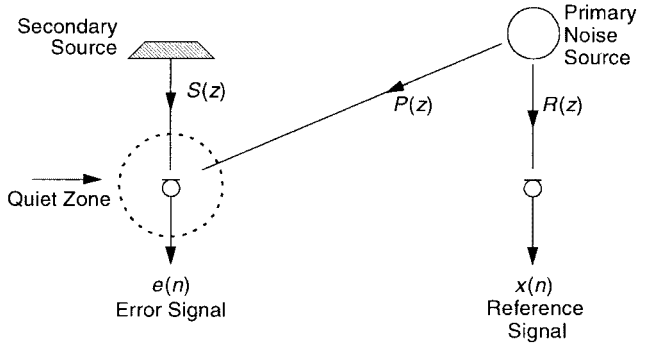

Fig. 32. Schematic diagram of acoustic ANC experiment in a reverberant room (adapted from [132]).

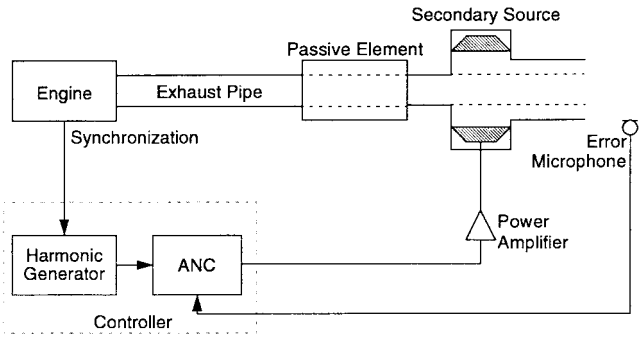

Fig. 33. Block diagram of electronic muffler (adapted from [141]).

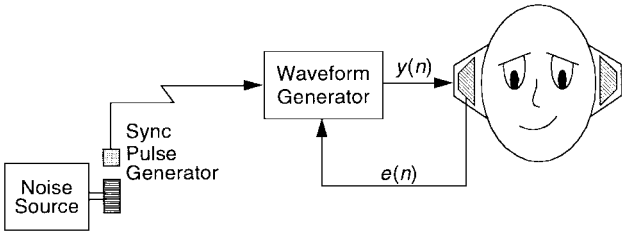

Fig. 34. Active headset for canceling narrow-band periodic noise (adapted from [142]).

obtains the error signal $e(n)$ which is to be minimized. The reference signal $x(n)$ is derived from another microphone on the right, which is in close proximity to the primary disturbance.

The application of ANC to the cancellation of broadband acoustic noise in a reverberant room requires a large number of taps. In order to minimize the computational rate and to enable the realization of this technique using a single low-cost DSP chip, the subband technique shown in Fig. 30 can be used. Application of this technique using a 512-tap wideband filter has achieved more than 15 dB of cancellation over a band of 100–500 Hz [132].

B. Single-Channel Narrow-Band Feedforward Systems

1) Engine Exhaust Noise: The characteristics of engine-generated noise can vary rapidly with abrupt changes in engine loading, such as when the engine is quickly accelerated or decelerated. In addition, engine-generated noise is dominated by harmonically related components having frequencies that vary as a function of the engine rotational speed. The dominant harmonic components will depend on the number of cylinders, due to the differing firing patterns.

An example of electronic muffler performance [140] was obtained for a 450-horsepower, six-cylinder, two-cycle diesel engine used to power an auxiliary electrical power generator. The multiple-frequency parallel FXLMS algorithm of Section III-D2 was used for this application. The electronic muffler eliminates the backpressure associated with a conventional passive muffler, even while reducing the noise level. The ANC system is normally limited to low-frequency operation; however, it can be combined with a low-pressure-drop passive silencer to attenuate the residual noise at higher frequencies. Thus, the combination is able to achieve both aims of low pressure drop and low noise, simultaneously.

The block diagram of the electronic muffler developed in [141] is shown in Fig. 33. Two 4.5-in low-frequency, high-temperature loudspeakers are used. The canceling noise is ported around the pipe in a coaxial arrangement, and cancellation takes place in the open air at the end of the pipe. The error microphone was mounted on the rear of the vehicle, 10 in from the end pipe. The system consists of three major subsystems discussed in Section III-C. The first is the waveform generator, which converts the pulse train from the engine tachometer into a set of sinewaves having frequencies that are multiples of the engine rotation rate. In the next subsystem, these sine waves are adaptively filtered (to adjust amplitude and phase) and then mixed to drive the canceling loudspeaker. The third subsystem monitors the residual noise at the control location and adapts the filter coefficients.

2) ANC Headsets: The purpose of hearing protectors is to protect the ear from harmful noise. The application of feedforward ANC using the waveform synthesis method has been developed [142] to cancel repetitive background noise at the ears of a person while retaining the ability to hear other ambient sounds, as illustrated in Fig. 34. The synchronization signals can be obtained by either optical, ultrasonic, or electrical means (e.g., wire or radio). The synchronization system can be common to a number of ANC headsets, such as in the case of a vehicle carrying multiple passengers. Because the cancellation only affects noise synchronized to the source of the repetitive background noise, most of the low-frequency sound that is not synchronized remains unaffected.

3) Fan Noise: A single-channel narrow-band ANC system can be used to cancel noise radiated from small axial flow fans. One such application appears in [143], which uses an infrared detector placed over the fan to derive blade passage rate. Experiments showed that the radiation of blade passage tones could be attenuated by 12 dB using this method. The development of an ANC system for ducted fans using the waveform synthesis method has also been reported [144], [145].

C. Multiple-Channel Feedforward Systems

Multiple-channel feedforward ANC applications have been demonstrated for vibration ANC on mechanical structures, acoustic ANC in enclosures such as automobile and aircraft cabins, free-field transformer noise, and acoustic ANC in large-dimensional ducts with high-order modes.

1) Vehicle Enclosures: Most midsize four-cylinder vehicles suffer from engine noise, particularly the low frequency "boom" at the engine firing frequency, which is the dominant source of internal noise at higher engine speeds [82]. With respect to the interior space of automobiles, three aspects can be considered beneficial for the success of ANC: 1) the periodicity of engine-related noise; 2) the relatively small volume of the cabin, which leads to a small overlap of the resonant modes in the lower frequency range; and 3) the fact that ANC is only required in the space where the heads of the driver and passenger are typically located. Therefore, a low-cost solution is to provide a quiet zone inside the cabin around the driver's and passengers' head position.

Engine-related narrow-band noise components can be canceled either by the waveform synthesis method or by the adaptive notch filter technique. The engine speed is measured by an electrical sensor, providing a pulse sequence from which a reference signal is synthesized. The canceling signal is generated by an adaptive filter that feeds secondary loudspeakers serving as control sources. A fast algorithm to adapt the adaptive filter coefficients is essential to provide a canceling signal that tracks under rapidly changing ride conditions. Therefore, an ANC system in a cabin will continue to function even when windows or hatches are opened, and therefore enables external warning sounds to be heard.

Elliott and coworkers developed an ANC system for the reduction of engine noise in a car [33], [81]. In this system, a reference signal was obtained from the ignition circuit and six loudspeakers in the car were used. These loudspeakers and their associated power amplifiers can be shared with the in-car entertainment system. Up to eight error microphones were used to monitor the performance of the ANC system. A reduction of 10–15 dB at the engine firing frequency was achieved by this ANC system.

Active control of low-frequency road noise presents a greater challenge than controlling engine noise. In that application, multiple broad-band primary noises require higher-order adaptive filters, thus considerably increasing the convergence time and computational burden. In one application [146], six accelerometers were placed close to the front wheels. Two secondary loudspeakers were placed in the doors adjacent to the driver and front passenger, and two error microphone were placed on the front headrests at the outer ear positions. The multiple-channel FXLMS algorithm discussed in Section V-B was used for this application. A broad-band reduction of about 7 dB (A-weighted) in the sound pressure level was measured when driving on a typical road surface. In this application, the important design issues are the placement of reference sensors for maximum coherence with respect to the interior noise to be canceled and the time delay of the reference signals.

Vibrational ANC in automobiles is a simple extension of acoustic ANC [82]. Accelerometers and actuators are located on the chassis side of active engine mounts. The potential benefits of active engine mounts are very dramatic, not only reducing acoustic noise and mechanical vibration within the cabin but also improving the control and ride qualities of the vehicle.

2) Aircraft Cabins: The interior noise of propeller-driven aircraft was found to be dominated by tones at the fundamental and harmonic frequencies of the propeller. Feedforward ANC systems with 16 loudspeakers and 32 microphones have been developed for noise control in the passenger cabin of a propeller aircraft [88]. The 32 microphones are located at seated head height throughout the passenger cabin. An alternative technique for controlling aircraft interior noise is to use lightweight vibrational secondary sources on the fuselage [147], [148].

3) Free-Field Radiation: In many situations, undesired noise is radiated into the far field. If the noise source is fixed and well defined, it is possible to suppress the radiation scattered by the primary noise source by surrounding the noise source with a layer of secondary sources. This concept is known as an active noise barrier. The ANC technique can be combined with a passive barrier in order to improve the noise attenuation at low frequencies. The location and separation of the error sensors and secondary sources can be optimized to get large noise attenuation over a wide area. A configuration of two independent $1 \times 4 \times 4$ systems was tested in [149] using the narrow-band multiple-channel FXLMS algorithm. A cancellation of 6–30 dB was demonstrated over a wide area. To obtain greater spatial coverage, it is necessary to deploy a system with more channels. Potential applications of this technique are reducing environmental noise in local areas, such as quieting the position of a machine operator in a noisy factory, providing a noise screen for a bed at an airport hotel, creating a noise barrier at airports, highways, and so on.

4) Transformer Noise: ANC also offers an alternative to large passive barriers for attenuating transformer noise [150]. This noise is composed of even-numbered harmonics of the 60-Hz power frequency. Experiments using four secondary loudspeakers and six error microphones with the $1 \times 4 \times 6$ narrow-band FXLMS algorithm have shown that sparse arrays of cancelers are effective in providing attenuation over significant angles of azimuth. Cancellation values of 15–20 dB were obtained over 35–40° of azimuth at 120 Hz, and 12–15 dB over 15–35° of azimuth at 240 Hz [150]. A similar system composed of three controllers, three microphones, and three loudspeakers has been developed [151], and more than 10-dB sound pressure level reduction was achieved.

5) Integration with Audio and Communication Systems: As ANC continues to progress, the need for successful integration with existing systems becomes apparent. This expectation of a unified digital solution is exemplified

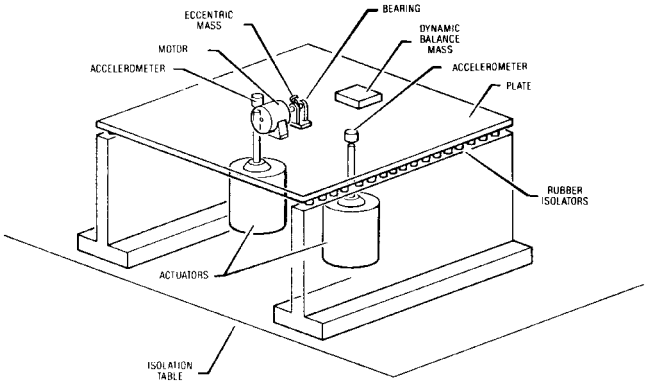

Fig. 35. Experimental structure for two-channel vibration ANC experiment (from [152]).

in modern automotive electronics. A unified approach to combine ANC, in-car entertainment, and communication (cellular phone) systems has been proposed [111] using an adaptive noise canceler to attenuate noise picked up by the microphone before transmission, an acoustic echo canceler to reduce acoustic echo from the loudspeaker to the microphone for hands-free full-duplex cellular phones, and a multiple-channel ANC system to reduce the acoustic noise inside an automobile passenger compartment.

It has been found that the standard in-car entertainment loudspeaker positions are often quite acceptable for ANC applications, while the error microphones can be distributed at positions determined by acoustic mode analysis of the vehicle [82]. Production vehicles will utilize the same loudspeakers as used by the in-car entertainment system, sharing the same power amplifier. The in-car entertainment system is moving to a completely digital system, in which case ANC may ultimately become a software addition to the digital audio system.

6) Modal ANC for a Vibrating Beam: The modal ANC concept introduced in Section VII-B is exemplified by the control of a vibrating cantilever beam [138]. The modes were calculated, and driving frequencies f_0 up to the sixth modal frequency were considered. For each frequency, four equally-spaced secondary sources were employed for cancellation. The resulting maximum achievable MSE reduction decreases as the frequency increases due to the presence of a greater number of contributing modes at higher frequencies.

7) Vibrating-Plate ANC: A single-channel pseudocascade FXLMS adaptive notch filter discussed in Section III-D4 was extended to the multiple-channel case [60]. Fig. 35 shows a sketch of a mechanical test structure that was assembled to study the effectiveness of the pseudocascade FXLMS algorithm for vibration ANC [152]. The structure consists of a 1/8-in steel plate mounted on vertical rubber isolators along two edges. Sensors and actuators are attached to the plate surface at optimum locations to monitor and counteract residual structural vibrations from the first and third vibrational modes.

A three-stage, two-channel pseudocascade FXLMS algorithm was implemented to control the actuators. The cancellation notch frequencies were selected at 13.38, 14.38, and 15.38 Hz, corresponding to the first modal resonance frequency flanked by two adjacent frequencies 1 Hz away. The three notches are able to carve out a relatively wide cancellation bandwidth to effectively suppress the disturbance.

8) Earth-Moving Machine: Experiments of multiple-channel acoustic ANC systems were conducted [153]–[155] for a typical earth-moving machine cabin. A $1 \times 2 \times 2$ system (one reference signal, two secondary sources, two error sensors) was implemented on a Texas Instruments TMS320C30 floating-point DSP chip for real-time experiments. The experimental setup of this multiple-channel ANC system consists of a real earth-moving machine cabin, as illustrated in Fig. 36. The setup utilizes two 10-in secondary loudspeakers mounted overhead. A reference microphone is located off the front wall, outside the cabin, centered laterally 35 cm above the floor plane. A multiple-channel ANC is implemented using the multiple-channel FXLMS algorithm discussed in Section V-B1. Two cardioid error microphones enhance the cancellation zone spatially by aiming the lobes of maximum sensitivity toward the quiet zone. Real engine noise was recorded at a position outside the cabin of an actual wheel loader. This noise was then reproduced outside of the test cabin through 15-in loudspeakers, at the location of the original recording, using a 300-W power amplifier. The sound pressure level of the reproduced noise was closely matched to that of the observed real engine noise.

The multiple-channel ANC system was operated to cancel noise inside the cabin in the vicinity of a normal operator's head position for several static test conditions. It was determined that the adaptive filter order $L = 256$ is near optimal not only for cancellation reasons, but also for achieving robust multiple-channel ANC performance. Filters of shorter length are not as robust against movements of people inside the enclosure or other factors, such as the opening or closing of the door or windows.

The FXLMS algorithm (Section V-B1), the FXLMS algorithm with feedback neutralization (Section V-B3), and the filtered-U recursive LMS algorithm (Section V-C) were implemented [154] using a TMS320C30 DSP chip. These ANC systems were tested with two different primary noises. First, a single sinewave was used as the primary noise. Next, the real engine noise recorded from the running diesel engine of an earth-moving machine was used as the primary noise for the ANC systems. The best sinusoidal noise cancellation is achieved using the filtered-U recursive LMS algorithm. However, when the primary noise is the actual recorded engine noise, the multiple-channel ANC system has about 20-dB attenuation for all three algorithms. This outcome stresses the importance of using real-world data.

D. Adaptive Feedback ANC Systems

1) Single-Channel Systems: Experiments were conducted in [97] for the single-channel feedback ANC system discussed in Section IV-A1, which uses one secondary source and one error sensor. The adaptive feedback ANC algorithm

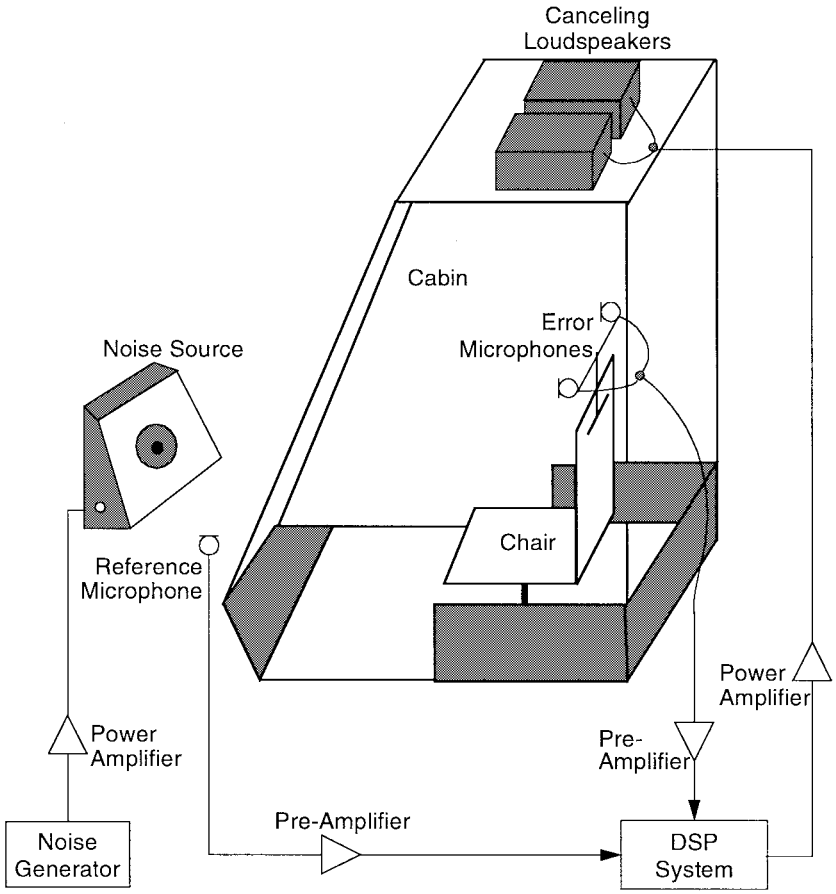

Fig. 36. Experimental setup for $1 \times 2 \times 2$ multiple-channel broad-band feedforward ANC system (adapted from [154]).

was implemented on a Texas Instruments TMS320C30-based system. The microphone that senses the residual error signal was placed on the axis of the pipe at various locations from the pipe exit. The convergence of the system depends on adjustment of the microphone preamplifier gain because the microphone signal is used to synthesize the reference signal. The adaptive feedback ANC system was tested using real noise recorded from a running tractor engine and about 30 dB of reduction of the harmonic components is achieved [156].

2) Multiple-Channel Systems: The multiple-channel feedback ANC algorithm was tested for a system with two secondary loudspeakers and one error microphone, the 2×1 case [97]. For such an arrangement, there are two secondary paths from the secondary loudspeakers to the error microphone. An experimental setup of the multiple-channel adaptive feedback ANC system utilized a wooden model of an open-rollover-protection tractor. The error microphone was positioned between and facing the two secondary loudspeakers mounted on the roof of the cabin. The noise source was a loudspeaker placed on the floor about 2 ft in front of the seat. The experimental setup is similar to Fig. 36, except that there is no reference microphone in the adaptive feedback ANC system.

The performance of the 2×1 adaptive feedback ANC system was tested using recorded tractor engine noise. On the average, about 20 dB attenuation was obtained for most of the significant harmonics present in the primary noise. The experimental setup for the 2×2 case is similar to that for the 2×1 case except that two error microphones are used. The secondary loudspeakers were again mounted on the roof of the cabin and the two error microphones were placed below and facing the two loudspeakers. The performance of the 2×2 adaptive feedback ANC system is similar to that of the 2×1 system.

IX. Conclusions

ANC cancels the unwanted noise by generating antinoise of equal amplitude and opposite phase through the secondary sources. This paper has emphasized the practical aspects of ANC systems in terms of adaptive algorithms and DSP implementations for real-world applications. The most widely used ANC system with the adaptive transversal filter and the FXLMS algorithm was first developed and analyzed based on single-channel cases for broad-band feedforward, narrow-band feedforward, and adaptive feedback control. These single-channel ANC algorithms were then expanded to multiple-channel cases for controlling the noise field in an enclosure or a large-dimension duct. Various adaptive algorithms such as the lattice, frequency-domain, subband, and RLS algorithms were also modified for ANC applications. The fundamental problems and several solutions

to online secondary-path modeling were discussed for providing some directions on new algorithm developments. Application examples demonstrated the connection to real-world problems.

REFERENCES

[1] C. M. Harris, *Handbook of Acoustical Measurements and Noise Control*, 3rd ed. New York: McGraw-Hill, 1991.

[2] L. L. Beranek and I. L. Ver, *Noise and Vibration Control Engineering: Principles and Applications*. New York: Wiley, 1992.

[3] P. A. Nelson and S. J. Elliott, *Active Control of Sound*. San Diego, CA: Academic, 1992.

[4] S. M. Kuo and D. R. Morgan, *Active Noise Control Systems—Algorithms and DSP Implementations*. New York: Wiley, 1996.

[5] C. R. Fuller, S. J. Elliott, and P. A. Nelson, *Active Control of Vibration*. San Diego, CA: Academic, 1996.

[6] C. H. Hansen and S. D. Snyder, *Active Control of Noise and Vibration*. London, U.K.: E&FN Spon, 1997.

[7] P. Lueg, "Process of silencing sound oscillations," U.S. Patent 2 043 416, June 9, 1936.

[8] G. C. Goodwin and K. S. Sin, *Adaptive Filtering Prediction and Control*. Englewood Cliffs, NJ: Prentice-Hall, 1984.

[9] B. Widrow and S. D. Stearns, *Adaptive Signal Processing*. Englewood Cliffs, NJ: Prentice-Hall, 1985.

[10] C. F. N. Cowan and P. M. Grant, *Adaptive Filters*. Englewood Cliffs, NJ: Prentice-Hall, 1985.

[11] M. L. Honig and D. G. Messerschmitt, *Adaptive Filters: Structures, Algorithms, and Applications*. Boston, MA: Kluwer, 1986.

[12] S. T. Alexander, *Adaptive Signal Processing*. New York: Springer-Verlag, 1986.

[13] J. R. Treichler, C. R. Johnson, Jr., and M. G. Larimore, *Theory and Design of Adaptive Filters*. New York: Wiley, 1987.

[14] M. Bellanger, *Adaptive Digital Filters and Signal Analysis*. New York: Marcel Dekker, 1987.

[15] S. Haykin, *Adaptive Filter Theory*, 2nd ed. Englewood Cliffs, NJ: Prentice-Hall, 1991.

[16] P. M. Clarkson, *Optimal and Adaptive Signal Processing*. Boca Raton, FL: CRC Press, 1993.

[17] J. C. Burgess, "Active adaptive sound control in a duct: A computer simulation," *J. Acoust. Soc. Amer.*, vol. 70, pp. 715–726, Sept. 1981.

[18] G. E. Warnaka, J. Tichy, and L. A. Poole, "Improvements in adaptive active attenuators," in *Proc. Inter-noise*, 1981, pp. 307–310.

[19] K. Kido, "Reduction of noise by use of additional sound sources," in *Proc. Inter-noise*, 1975, pp. 647–650.

[20] C. F. Ross, "A demonstration of active control of broadband sound," *J. Sound Vib.*, vol. 74, no. 3, pp. 411–417, 1981.

[21] S. M. Kuo and C. Chen, "Implementation of adaptive filters with the TMS320C25 or the TMS320C30," in *Digital Signal Processing Applications with the TMS320 Family*, vol. 3, P. Papamichalis, Ed. Englewood Cliffs, NJ: Prentice-Hall, 1990, ch. 7, pp. 191–271.

[22] L. J. Eriksson, "Computer-aided silencing—An emerging technology," *Sound Vib.*, vol. 24, pp. 42–45, July 1990.

[23] M. Nishimura, "Some problems of active noise control for practical use," in *Proc. Int. Symp. Active Control of Sound Vibration*, 1991, pp. 157–164.

[24] D. R. Morgan, "A hierarchy of performance analysis techniques for adaptive active control of sound and vibration," *J. Acoust. Soc. Amer.*, vol. 89, pp. 2362–2369, May 1991.

[25] A. Roure, "Self-adaptive broadband active sound control system," *J. Sound Vib.*, vol. 101, pp. 429–441, 1985.

[26] H. F. Olson and E. G. May, "Electronic sound absorber," *J. Acoust. Soc. Amer.*, vol. 25, pp. 1130–1136, Nov. 1953.

[27] H. F. Olson, "Electronic control of noise, vibration, and reverberation," *J. Acoust. Soc. Am.*, vol. 28, pp. 966–972, Sept. 1956.

[28] G. C. Carter, "Coherence and time delay estimation," *Proc. IEEE*, vol. 75, pp. 236–255, Feb. 1987.

[29] S. M. Kuo and J. Tsai, "Acoustical mechanisms and performance of various active duct noise control systems," *Appl. Acoust.*, vol. 41, no. 1, pp. 81–91, 1994.

[30] S. J. Elliott and P. A. Nelson, "The application of adaptive filtering to the active control of sound and vibration," ISVR, Univ. Southampton, U.K., Tech. Rep. 136, Sept. 1985.

[31] D. R. Morgan, "An analysis of multiple correlation cancellation loops with a filter in the auxiliary path," *IEEE Trans. Acoust., Speech, Signal Processing*, vol. ASSP-28, pp. 454–467, Aug. 1980.

[32] B. Widrow, D. Shur, and S. Shaffer, "On adaptive inverse control," in *Proc. 15th Asilomar Conf.*, 1981, pp. 185–189.

[33] S. J. Elliott and P. A. Nelson, "Active noise control," *IEEE Signal Processing Mag.*, vol. 10, pp. 12–35, Oct. 1993.

[34] C. C. Boucher, S. J. Elliott, and P. A. Nelson, "The effects of modeling errors on the performance and stability of active noise control systems," in *Proc. Recent Advances in Active Control of Sound Vibration*, 1991, pp. 290–301.

[35] ——, "Effect of errors in the plant model on the performance of algorithms for adaptive feedforward control," *Proc. Inst. Elect. Eng.*, pt. F, vol. 138, pp. 313–319, Aug. 1991.

[36] S. D. Snyder and C. H. Hansen, "The effect of transfer function estimation errors on the filtered-X LMS algorithm," *IEEE Trans. Signal Processing*, vol. 42, pp. 950–953, Apr. 1994.

[37] G. Long, F. Ling, and J. G. Proakis, "The LMS algorithm with delayed coefficient adaptation," *IEEE Trans. Acoust., Speech, Signal Processing*, vol. 37, pp. 1397–1405, Sept. 1989.

[38] ——, "Corrections to 'The LMS algorithm with delayed coefficient adaptation'," *IEEE Trans. Signal Processing*, vol. 40, pp. 230–232, Jan. 1992.

[39] S. J. Elliott, I. M. Stothers, and P. A. Nelson, "A multiple error LMS algorithm and its application to the active control of sound and vibration," *IEEE Trans. Acoust., Speech, Signal Processing*, vol. ASSP-35, pp. 1423–1434, Oct. 1987.

[40] R. D. Gitlin, H. C. Meadors, and S. B. Weinstein, "The tap-leakage algorithm: An algorithm for the stable operation of a digitally implemented, fractionally spaced adaptive equalizer," *Bell Syst. Tech. J.*, vol. 61, pp. 1817–1839, Oct. 1982.

[41] S. Laugesen and S. J. Elliott, "Multichannel active control of random noise in a small reverberant room," *IEEE Trans. Signal Processing*, vol. 1, pp. 241–249, Apr. 1993.

[42] P. R. Enderle and G. R. Batta, "Stability of active noise control systems in ducts," in *Proc. Noise-Con*, 1990, pp. 167–172.

[43] M. M. Sondhi and D. A. Berkley, "Silencing echoes on the telephone network," *Proc. IEEE*, vol. 68, pp. 948–963, Aug. 1980.

[44] L. A. Poole, G. E. Warnaka, and R. C. Cutter, "The implementation of digital filter using a modified Widrow-Hoff algorithm for the adaptive cancellation of acoustic noise," in *Proc. ICASSP*, 1984, pp. 21.7.1–21.7.4.

[45] J. R. Treichler, "Adaptive algorithms for infinite impulse response filters," in *Adaptive Filters*, C. F. N. Cowan and P. M. Grant, Eds. Englewood Cliffs, NJ: Prentice-Hall, 1985, ch. 4.

[46] J. J. Shynk, "Adaptive IIR filtering," *IEEE Acoust. Speech Signal Processing Mag.*, Apr. 1989, pp. 4–21.

[47] L. J. Eriksson, M. C. Allie, and R. A. Greiner, "The selection and application of an IIR adaptive filter for use in active sound attenuation," *IEEE Trans. Acoust., Speech, Signal Processing*, vol. ASSP-35, pp. 433–437, Apr. 1987.

[48] P. L. Feintuch, "An adaptive recursive LMS filter," *Proc. IEEE*, vol. 64, pp. 1622–1624, Nov. 1976.

[49] L. J. Eriksson, "Development of the filtered-U algorithm for active noise control," *J. Acoust. Soc. Amer.*, vol. 89, pp. 257–265, Jan. 1991.

[50] M. L. Munjal and L. J. Eriksson, "An analytical, one-dimensional, standing-wave model of a linear active noise control system in a duct," *J. Acoust. Soc. Amer.*, vol. 84, pp. 1086–1093, Sept. 1988.

[51] L. J. Eriksson, M. C. Allie, C. D. Bremigan, and J. A. Gilbert, "Active noise control on systems with time-varying sources and parameters," *Sound Vibration*, vol. 23, pp. 16–21, July 1989.

[52] M. G. Larimore, J. R. Treichler, and C. R. Johnson, Jr., "SHARF: An algorithm for adaptive IIR digital filters," *IEEE Trans. Acoust., Speech, Signal Processing*, vol. ASSP-28, pp. 428–440, Aug. 1980.

[53] S. M. Kuo and J. Tapia, "The implementation of modified leaky SHARF algorithm for the active noise cancellation," in *Proc. IEEE ASSP Workshop Applications of Signal Processing to Audio and Acoustics*, 1989.

[54] S. J. Elliott and P. Darlington, "Adaptive cancellation of periodic, synchronously sampled interference," *IEEE Trans.*

Acoust., Speech, Signal Processing, vol. ASSP-33, pp. 715–717, June 1985.
[55] B. Chaplin, "The cancellation of repetitive noise and vibration," in *Proc. Inter-noise*, 1980, pp. 699–702.
[56] B. Widrow, J. R. Glover, J. M. McCool, J. Kaunitz, C. S. Williams, R. H. Hern, J. R. Zeidler, E. Dong, and R. C. Goodlin, "Adaptive noise canceling: Principles and applications," *Proc. IEEE*, vol. 63, pp. 1692–1716, Dec. 1975.
[57] E. Ziegler, Jr., "Selective active cancellation system for repetitive phenomena," U.S. Patent 4 878 188, Oct. 31, 1989.
[58] P. Darlington and S. J. Elliott, "Stability and adaptively controlled systems—A graphical approach," in *Proc. ICASSP*, 1987, pp. 399–402.
[59] ——, "Synchronous adaptive filters with delayed coefficient adaptation," in *Proc. ICASSP*, 1988, pp. 2586–2589.
[60] D. R. Morgan and J. Thi, "A multitone pseudocascade filtered-X LMS adaptive notch filter," *IEEE Trans. Signal Processing*, vol. 41, pp. 946–956, Feb. 1993.
[61] J. R. Glover, Jr., "Adaptive noise canceling applied to sinusoidal interferences," *IEEE Trans. Acoust., Speech, Signal Processing*, vol. ASSP-25, pp. 484–491, Dec. 1977.
[62] D. R. Morgan and C. Sanford, "A control theory approach to the stability and transient analysis of the filtered-X LMS adaptive notch filter," *IEEE Trans. Signal Processing*, vol. 40, pp. 2341–2346, Sept. 1992.
[63] S. M. Kuo and M. Ji, "Passband disturbance reduction in periodic active noise control systems," *IEEE Trans. Speech Audio Processing*, vol. 4, pp. 96–103, Mar. 1996.
[64] S. M. Kuo, S. Zhu, and M. Wang, "Development of optimum adaptive notch filter for fixed-point implementation in active noise control," in *Proc. 1992 Int. Conf. Industrial Electronics*, 1992, pp. 1376–1378.
[65] D. P. Pfaff, N. S. Kapsokavathis, and N. A. Parks, "Method for actively attenuating engine generated noise," U.S. Patent 5 146 505, Sept. 8, 1992.
[66] Y. Yuan, N. S. Kapsokavathis, K. Chen, and S. M. Kuo, "Active noise control system," U.S. Patent 5 359 662, Oct. 25, 1994.
[67] S. M. Kuo, M. J. Ji, M. K. Christensen, and R. A. Herold, "Indirectly sensed signal processing in active periodic acoustic noise cancellation," U.S. Patent 5 502 770, Mar. 26, 1996.
[68] P. D. Hill, "Active acoustic attenuation system for reducing tonal noise in rotating equipment," U.S. Patent 5 010 576, Apr. 23, 1991.
[69] S. M. Kuo and M. J. Ji, "Development and analysis of an adaptive noise equalizer," *IEEE Trans. Speech Audio Processing*, vol. 3, pp. 217–222, May 1995.
[70] S. M. Kuo, M. Tahernezhadi, and L. Ji, "Frequency-domain periodic active noise control and equalization," *IEEE Trans. Speech Audio Processing*, vol. 5, pp. 348–358, July 1997.
[71] S. M. Kuo and Y. Yang, "Broadband adaptive noise equalizer," *IEEE Signal Processing Lett.*, vol. 3, pp. 234–235, Aug. 1996.
[72] L. J. Eriksson, "Recursive algorithms for active noise control," in *Proc. Int. Symp. Active Control of Sound Vibration*, 1991, pp. 137–146.
[73] S. R. Popovich, D. E. Melton, and M. C. Allie, "New adaptive multi-channel control systems for sound and vibration," in *Proc. Inter-noise*, 1992, pp. 405–408.
[74] S. M. Kuo and D. Vijayan, "Adaptive feedback active noise control," in *Proc. Noise-Con*, 1994, pp. 473–478.
[75] S. J. Elliott and T. J. Sutton, "Performance of feedforward and feedback systems for active control," *IEEE Trans. Speech Audio Processing*, vol. 4, pp. 214–223, May 1996.
[76] D. Graupe and A. J. Efron, "An output-whitening approach to adaptive active noise cancellation," *IEEE Trans. Circuits Syst. II*, vol. 38, pp. 1306–1313, Nov. 1991.
[77] A. J. Efron and L. C. Han, "Wide-area adaptive active noise cancellation," *IEEE Trans. Circuits Syst. II*, vol. 41, pp. 405–409, June 1994.
[78] A. V. Oppenheim, E. Weinstein, K. C. Zangi, M. Feder, and D. Gauger, "Single-sensor active noise cancellation," *IEEE Trans. Speech Audio Processing*, vol. 2, pp. 285–290, Apr. 1994.
[79] K. C. Zangi, "A new two-sensor active noise cancellation algorithm," in *Proc. ICASSP*, vol. II, 1993, pp. 351–354.
[80] D. C. Swanson, "Active noise attenuation using a self-tuning regulator as the adaptive control algorithm," in *Proc. Inter-noise*, 1989, pp. 467–470.
[81] S. J. Elliott, I. M. Stothers, P. A. Nelson, A. M. McDonald, D. C. Quinn, and T. Saunders, "The active control of engine noise inside cars," in *Proc. Inter-noise*, 1988, pp. 987–990.
[82] A. M. McDonald, S. J. Elliott, and M. A. Stokes, "Active noise and vibration control within the automobile," in *Proc. Int. Symp. Active Control of Sound Vibration*, 1991, pp. 147–156.
[83] Y. Kurata and N. Koike, "Adaptive active attenuation of interior car noise," in *Proc. Int. Symp. Active Control of Sound Vibration*, 1991, pp. 297–302.
[84] C. F. Ross, "The control of noise inside passenger vehicles," in *Proc. Recent Advances in Active Control of Sound Vibration*, 1991, pp. 671–681.
[85] S. M. Kuo and B. M. Finn, "A general multi-channel filtered LMS algorithm for 3-D active noise control systems," in *Proc. 2nd Int. Conf. Recent Developments in Air- and Structure-Borne Sound Vib.*, 1992, pp. 345–352.
[86] M. A. Simpson, T. M. Luong, M. A. Swinbanks, M. A. Russell, and H. G. Leventhall, "Full scale demonstration tests of cabin noise reduction using active noise control," in *Proc. Inter-noise*, 1989, pp. 459–462.
[87] C. M. Dorling, G. P. Eatwell, S. M. Hutchins, C. F. Ross, and S. G. C. Sutcliffe, "A demonstration of active noise reduction in an aircraft cabin," *J. Sound Vibration*, vol. 128, no. 2, pp. 358–360, 1989.
[88] S. J. Elliott, P. A. Nelson, I. M. Stothers, and C. C. Boucher, "In-flight experiments on the active control of propeller-induced cabin noise," *J. Sound Vibration*, vol. 140, no. 2, pp. 219–238, 1990.
[89] P. A. Nelson, A. R. D. Curtis, S. J. Elliott, and A. J. Bullmore, "The active minimization of harmonic enclosed sound fields, Part I: Theory," *J. Sound Vibration*, vol. 117, no. 1, pp. 1–13, 1987.
[90] A. J. Bullmore, P. A. Nelson, A. R. D. Curtis, and S. J. Elliott, "The active minimization of harmonic enclosed sound fields, Part II: A computer simulation," *J. Sound Vibration*, vol. 117, no. 1, pp. 15–33, 1987.
[91] S. J. Elliott, A. R. D. Curtis, A. J. Bullmore, and P. A. Nelson, "The active minimization of harmonic enclosed sound fields, Part III: Experimental verification," *J. Sound Vibration*, vol. 117, no. 1, pp. 35–58, 1987.
[92] S. J. Elliott, C. C. Boucher, and P. A. Nelson, "The behavior of a multiple channel active control system," *IEEE Trans. Signal Processing*, vol. 40, pp. 1041–1052, May 1992.
[93] P. A. Nelson, A. R. D. Curtis, S. J. Elliott, and A. J. Bullmore, "The minimum power output of free field point sources and the active control of sound," *J. Sound Vibration*, vol. 116, no. 3, pp. 397–414, 1987.
[94] D. C. Swanson, "The generalized multichannel filtered-X algorithm," in *Proc. Recent Advances in Active Control of Sound Vibration*, 1993, pp. 550–561.
[95] S. J. Elliott and C. C. Boucher, "Interaction between multiple feedforward active control systems," *IEEE Trans. Speech Audio Processing*, vol. 2, pp. 521–530, Oct. 1994.
[96] D. E. Melton and R. A. Greiner, "Adaptive feedforward multiple-input, multiple-output active noise control," in *Proc. ICASSP*, vol. II, 1992, pp. 229–232.
[97] S. M. Kuo and D. Vijayan, "Adaptive algorithms and experimental verification of feedback active noise control systems," *Noise Control Eng. J.*, vol. 42, pp. 37–46, Mar.–Apr. 1994.
[98] S. P. Rubenstein, S. R. Popovich, D. E. Melton, and M. C. Allie, "Active cancellation of higher modes in a duct using recursively-coupled multichannel adaptive control system," in *Proc. Inter-noise*, 1992, pp. 337–340.
[99] L. J. Eriksson and M. C. Allie, "Use of random noise for on-line transducer modeling in an adaptive active attenuation system," *J. Acoust. Soc. Amer.*, vol. 85, pp. 797–802, Feb. 1989.
[100] C. Bao, P. Sas, and H. Van Brussel, "Adaptive active noise control in a 3-D reverberant enclosure," in *Proc. Recent Advances in Active Control of Sound Vibration*, 1991, pp. 691–707.
[101] ——, "Adaptive active control of noise in 3-D reverberant enclosures," *J. Sound Vibration*, vol. 161, no. 3, pp. 501–514, 1993.
[102] S. M. Kuo and D. Vijayan, "A secondary path modeling technique for active noise control systems," *IEEE Trans. Speech Audio Processing*, vol. 5, pp. 374–377, July 1997.
[103] S. D. Sommerfeldt and J. Tichy, "Adaptive vibration control using an LMS-based control algorithm," in *Proc. Inter-noise*, 1989, pp. 513–518.
[104] ——, "Adaptive control of a two-stage vibration isolation mount," *J. Acoust. Soc. Amer.*, vol. 88, pp. 938–944, Aug. 1990.
[105] J. Tapia and S. M. Kuo, "New adaptive on-line modeling

technique for active noise control systems," in *Proc. IEEE Int. Conf. Systems Engineering*, 1990, pp. 280–283.
[106] S. M. Kuo and M. Wang, "Parallel adaptive on-line error-path modeling algorithm for active noise control systems," *Electron. Lett.*, vol. 28, pp. 375–377, Feb. 1992.
[107] S. M. Kuo, M. Wang, and K. Chen, "Active noise control system with parallel on-line error path modeling algorithm," *Noise Control Eng. J.*, vol. 39, pp. 119–127, Nov.–Dec. 1992.
[108] S. M. Kuo and J. Luan, "Multiple-channel error path modeling with the inter-channel decoupling algorithm," in *Proc. Recent Advances in Active Control of Sound Vibration*, 1993, pp. 767–777.
[109] S. D. Sommerfeldt, "Multi-channel adaptive control of structural vibration," *Noise Control Eng. J.*, vol. 37, pp. 77–89, Sept.–Oct., 1991.
[110] S. M. Kuo and B. M. Finn, "An integrated audio and active noise control system," in *Proc. IEEE Int. Symp. Circuits Syst.*, 1993, pp. 2529–2532.
[111] S. M. Kuo, H. Chuang, and P. Mallela, "Integrated hands-free cellular, active noise control, and audio system," *IEEE Trans. Consumer Electron.*, vol. 39, pp. 522–532, Aug. 1993.
[112] R. W. Harris, D. M. Chabries, and F. A. Bishop, "A variable step (VS) adaptive filter algorithm," *IEEE Trans. Acoust., Speech, Signal Processing*, vol. ASSP-34, pp. 309–316, Apr. 1986.
[113] C. Kwong, "Dual sign algorithm for adaptive filtering," *IEEE Trans. Commun.*, vol. COM-34, pp. 1272–1275, Dec. 1986.
[114] W. B. Mikhael, F. H. Wu, L. G. Kazovsky, G. S. Kang, and L. J. Fransen, "Adaptive filters with individual adaptation of parameters," *IEEE Trans. Circuits Syst.*, vol. CAS-33, pp. 677–685, July 1986.
[115] T. J. Shan and T. Kailath, "Adaptive algorithms with an automatic gain control feature," *IEEE Trans. Circuits Syst.*, vol. CAS-35, pp. 122–127, Jan. 1988.
[116] H. Hamada, T. Miura, M. Takahashi, and Y. Oguri, "Adaptive noise control system in air-conditioning ducts," in *Proc. Internoise*, 1988, pp. 1017–1020.
[117] M. Takahashi, R. Gotohda, T. Yamadera, K. Asami, and H. Hamada, "Broadband active noise control of air-conditioning duct systems in auditoriums," in *Proc. Int. Symp. Active Control of Sound Vibration*, 1991, pp. 273–278.
[118] L. J. Griffiths, "A continuously adaptive filter implemented as a lattice structure," in *Proc. ICASSP*, 1977, pp. 683–686.
[119] ——, "An adaptive lattice structure for noise canceling applications," in *Proc. ICASSP*, 1978, pp. 87–90.
[120] S. M. Kuo and J. Luan, "Cross-coupled filtered-X LMS algorithm and lattice structure for active noise control systems," in *Proc. 1993 IEEE Int. Symp. Circuits Systems*, 1993, pp. 459–462.
[121] K. Char and S. M. Kuo, "Performance evaluation of various active noise control algorithms," in *Proc. Noise-Con*, 1994, pp. 331–336.
[122] M. Dentino, J. M. McCool, and B. Widrow, "Adaptive filtering in the frequency domain," *Proc. IEEE*, vol. 66, pp. 1658–1659, Dec. 1978.
[123] E. R. Ferrara, Jr., "Frequency-domain adaptive filtering," in *Adaptive Filtering*, C. Cowan and P. Grant, Eds. Englewood Cliffs, NJ: Prentice-Hall, 1985, ch. 6.
[124] N. Ahmed, T. Natarajan, and K. R. Rao, "Discrete cosine transform," *IEEE Trans. Comput.*, vol. C-23, pp. 90–93, 1974.
[125] R. N. Bracewell, "The fast Hartley transform," *Proc. IEEE*, vol. 72, pp. 1010–1018, Aug. 1984.
[126] Q. Shen and A. Spanias, "Time and frequency domain X-block LMS algorithms for single channel active noise control," in *Proc. 2nd Int. Congr. Recent Developments in Air- and Structure-Borne Sound Vibration*, 1992, pp. 353–360.
[127] K. M. Reichard and D. C. Swanson, "Frequency-domain implementation of the filtered-X algorithm with on-line system identification," in *Proc. Recent Advances in Active Control of Sound Vibration*, 1993, pp. 562–573.
[128] Q. Shen and A. Spanias, "Frequency-domain adaptive algorithms for multi-channel active sound control," in *Proc. Recent Advances in Active Control of Sound Vibration*, 1993, pp. 755–766.
[129] M. M. Sondhi and W. Kellermann, "Adaptive echo cancellation for speech signals," in *Advances in Speech Signal Processing*, S. Furui and M. Sondhi, Eds. New York: Marcel Dekker, 1992, ch. 11.
[130] J. J. Shynk, "Frequency-domain and multirate adaptive filtering," *IEEE Signal Processing Mag.*, vol. 9, pp. 14–37, Jan. 1992.
[131] J. Thi and D. R. Morgan, "Delayless subband active noise control," in *Proc. ICASSP*, vol. I, 1993, pp. 181–184.
[132] D. R. Morgan and J. Thi, "A delayless subband adaptive filter," *IEEE Trans. Signal Processing*, vol. 8, pp. 1819–1830, Aug. 1995.
[133] J. M. Cioffi and T. Kailath, "Fast, recursive-least-squares transversal filters for adaptive filtering," *IEEE Trans. Acoust., Speech, Signal Processing*, vol. ASSP-32, pp. 304–337, Apr. 1984.
[134] L. Meirovitch, *Introduction to Dynamics and Control*. New York: Wiley, 1985.
[135] L. Meirovitch, H. Baruh, and H. Oz, "Comparison of control techniques for large flexible systems," *J. Guid. Control Dyn.*, vol. 6, pp. 302–310, July–Aug. 1983.
[136] L. Meirovitch and H. Baruh, "Robustness of the independent modal-space control method," *J. Guid. Control Dyn.*, vol. 6, pp. 20–25, Jan.–Feb. 1983.
[137] H. Baruh and L. Silverberg, "Robust natural control of distributed systems," *J. Guid. Control Dyn.*, vol. 8, pp. 717–724, Nov.–Dec. 1985.
[138] D. R. Morgan, "An adaptive modal-based active control system," *J. Acoust. Soc. Amer.*, vol. 89, pp. 248–256, Jan. 1991.
[139] C. P. Nowicki, D. P. Mendat, and D. G. Smith, "Active attenuation of motor/blower noise," in *Proc. Noise-Con*, 1994, pp. 415–420.
[140] J. N. Denenberg, "Anti-noise—Quieting the environment with active noise cancellation technology," *IEEE Potentials*, vol. 11, pp. 36–40, Apr. 1992.
[141] K. Eghtesadi and E. Ziegler, "Frequency domain adaptive control algorithm for electronic muffler applications," in *Proc. Recent Advances in Active Control of Sound Vib.*, 1993, pp. 574–585.
[142] G. B. B. Chaplin, R. A. Smith, and T. P. C. Bramer, "Method and apparatus for reducing repetitive noise entering the ear," U.S. Patent 4 654 871, Mar. 31, 1987.
[143] D. A. Quinlan, "Application of active control to axial flow fans," *Noise Control Eng. J.*, vol. 39, pp. 95–101, Nov.–Dec. 1992.
[144] M. P. McLonghlin, K. Eghtesadi, D. G. Smith, and E. W. Ziegler, Jr., "Active control of blade passage noise in small centrifugal fans with multiple transducers," in *Proc. Inter-noise*, 1992, pp. 325–328.
[145] D. L. Sutliff and R. T. Nagel, "Development of an active noise control system for ducted fans (without acoustic feedback)," in *Proc. Recent Advances in Active Control of Sound Vib.*, 1993, pp. 825–836.
[146] T. J. Sutton, S. J. Elliott, A. M. McDonald, and T. J. Saunders, "Active control of road noise inside vehicles," *Noise Control Eng. J.*, vol. 42, pp. 137–147, July–Aug. 1994.
[147] C. R. Fuller and J. D. Jones, "Experiments on reduction of propeller induced interior noise by active control of cylinder vibration," *J. Sound Vib.*, vol. 112, pp. 389–395, 1987.
[148] C. R. Fuller and G. P. Gibbs, "Active control of interior noise in a business jet using piezoceramic actuators," in *Proc. Noise-Con*, 1994, pp. 389–394.
[149] A. Omoto and K. Fujiwara, "A study of an actively controlled noise barrier," *J. Acoust. Soc. Am.*, vol. 94, pp. 2173–2180, Oct. 1993.
[150] S. E. Craig and O. L. Angevine, "Active control of hum from large power transformers—The real world," in *Proc. Recent Advances in Active Control of Sound Vibration*, 1993, pp. 279–290.
[151] K. Kido, "From one point to three dimension control," in *Proc. Int. Symp. Active Control of Sound Vibration*, 1991, pp. 1–10.
[152] D. R. Browning and D. R. Morgan, "A pseudo-cascade FXLMS approach to active vibration cancellation," in *Proc. Noise-Con*, 1991, pp. 353–360.
[153] B. M. Finn, "Three dimensional active noise control with integrated audio capabilities," M.S. thesis, Northern Illinois Univ., DeKalb, IL. 1992.
[154] J. Luan, "On-line modeling and feedback compensation techniques for 3-d active noise control systems," M.S. thesis, Northern Illinois Univ., DeKalb, IL, May 1993.
[155] M. J. Ji, "Narrowband active noise control and equalization," M.S. thesis, Northern Illinois Univ., DeKalb, IL, Aug. 1993.

[156] D. Vijayan, Feedback active noise control systems, M.S. thesis, Northern Illinois Univ., DeKalb, IL, May 1994.

Sen M. Kuo received the B.S. degree from National Taiwan Normal University, Teipei, Taiwan, in 1976 and the M.S. and Ph.D. degrees from University of New Mexico, Albuquerque, in 1983 and 1985, respectively.

In 1993, he was with Texas Instruments, Houston, TX. He is currently an Associate Professor at the Department of Electrical Engineering, Northern Illinois University, DeKalb, IL. He has served as a consultant in the areas of digital signal processing applications to General Motors, Texas Instruments, Motorola, Tellabs, and others. He is the author of *Active Noise Control Systems: Algorithms and DSP Implementations* (New York: Wiley, 1996) and of numerous technical papers. He has been awarded two patents. His research focuses on active noise control, adaptive echo cancellation, digital audio applications, and digital communications.

In 1993, Dr. Kuo received the IEEE Consumer Electronics Society Chester Sall Award for the First Place Transactions Paper Award. He is a member of Eta Kappa Nu.

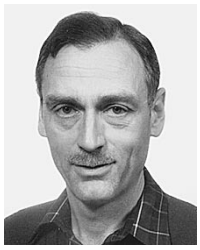

Dennis R. Morgan (Senior Member, IEEE) was born in Cincinnati, OH, on February 19, 1942. He received the B.S. degree in 1965 from the University of Cincinnati, OH, and the M.S. and Ph.D. degrees from Syracuse University, Syracuse, NY, in 1968 and 1970, respectively, all in electrical engineering.

From 1965 to 1984, he was with the General Electric Company, Electronics Laboratory, Syracuse, NY, specializing in the analysis and design of signal processing systems used in radar, sonar, and communications. He is now a Distinguished Member of Technical Staff at Bell Laboratories, Lucent Technologies (formerly AT&T), Murray Hill, NJ, where he has been employed since 1984. From 1984 to 1990, he was with the Special Systems Analysis Department, Whippany, NJ, where he was involved in the analysis and development of advanced signal processing techniques associated with communications, array processing, detection and estimation, and adaptive systems. Since 1990, he has been with the Acoustics Research Department, where he is engaged in research on adaptive signal processing techniques applied to electroacoustic systems. He has authored numerous journal publications and is co-athor of *Active Noise Control Systems: Algorithms and DSP Implementations* (New York: Wiley, 1996).

Dr. Morgan has served as Associate Editor for IEEE TRANSACTIONS ON SPEECH AND AUDIO PROCESSING since 1995.